Changes in productivity and intermediate circulation in the northern Indian Ocean since the last deglaciation: new insights from benthic foraminiferal Cd/Ca records and benthic assemblage analyses

Ruifang Ma[1,2*], Sophie Sépulcre[1], Laetitia Licari[3], Frédéric Haurine[1], Franck Bassinot[4], Zhaojie Yu[5], Christophe Colin[1]

[1] GEOPS, Université Paris-Saclay, CNRS, Orsay, 91405, France.
[2] State Key Laboratory of Cryospheric Science, Northwest Institute of Eco-Environment and Resources, Chinese Academy of Sciences, Lanzhou, 730000, China.
[3] CEREGE, Aix-Marseille Université-Europole de l'Arbois-BP80, Aix-en-Provence, 13545, France.
[4] LSCE/IPSL, CEA CNRS UVSQ, Gif Sur Yvette, F-91190, France.
[5] Key Laboratory of Marine Geology and Environment, Institute of Oceanology, Chinese Academy of Sciences, Qingdao, 266071, China.

*Correspondence to: R. MA (maruifang89@hotmail.com)

Abstract. We have measured Cd/Ca ratios of several benthic foraminiferal species and studied benthic foraminiferal assemblages on two cores from the northern Indian Ocean (Arabian Sea and northern Bay of Bengal, BoB), in order to reconstruct variations in intermediate water circulation and paleo-nutrient content since the last deglaciation. Intermediate water Cd_w records estimated from the benthic Cd/Ca reflect past changes in surface productivity and/or intermediate-bottom water ventilation. The benthic foraminiferal assemblages are consistent with the geochemical data. These results suggest that during the last deglaciation, the Heinrich Stadial 1 and Younger Dryas (HS1 and YD, respectively) millennial-scale events were marked by a decrease in Cd_w values, indicating an enhanced ventilation of intermediate-bottom water masses. During the early Holocene (from 10 to 6 cal kyr BP), bBenthic foraminiferal assemblages indicate that surface primary productivity was low during the early Holocene (from 10 to 6 cal kyr BP), resulting in low intermediate water Cd_w at both sites. Then, fFrom ~ 5.2 to 2.4 cal kyr BP, the benthic foraminiferal assemblages indicate meso- to eutrophic intermediate water conditions, which correspond to high surface productivity. This is consistent with a significant increase in the intermediate water Cd_w in the southeastern Arabian Sea and the northeastern BoB. The comparison of intermediate water Cd_w records with previous reconstructions of past Indian monsoon evolution during the Holocene suggests a direct control of intermediate water Cd_w by monsoon-induced changes in upper water stratification and surface primary productivity.

1. Introduction

During the last deglaciation, a two-step rapid increase in atmospheric CO_2 occurred during the 18-14.7 and 12.8-11.7 cal kyr BP time intervals (e.g., Monnin et al., 2001). Several studies suggest that variations in the Southern Ocean circulation contributed to these increases in atmospheric CO_2 by transferring deep ocean carbon to the upper ocean and atmosphere, through enhanced upwelling and increased northward penetration of the Antarctic Intermediate Water (AAIW) in all ocean basins (e.g., Marchitto et al., 2007; Anderson et al., 2009; Skinner et al., 2014). Different proxies have been used to reconstruct past changes in intermediate circulation,

41 such as radiocarbon activity ($\Delta^{14}C$) (e.g., Marchitto et al., 2007; Bryan et al., 2010), benthic $\delta^{13}C$ (e.g., Pahnke

42 and Zahn, 2005; Jung et al., 2009; Ma et al., 2019), foraminiferal ε_{Nd} (e.g., Pahnke et al., 2008; Xie et al., 2012;

43 Yu et al., 2018) and benthic foraminifera Sr/Ca (Ma et al., 2020). These studies have focused on the close

44 relationship between enhanced ventilation in the Southern Ocean and rising atmospheric CO_2 during the last

45 deglaciation period. Furthermore, it has been shown that glacial-interglacial transfer of CO_2 between the oceans

46 and the atmosphere could also be linked to changes in the efficiency of the oceanic biological pump (Pichevin et

47 al., 2009; Ziegler et al., 2013; Bauska et al., 2016; Hertzberg et al., 2016; Jaccard et al., 2016; Yu et al., 2019),

48 which may contribute up to half of the observed CO_2 flux (Kohfeld, 2005).

49   The oceanic biological pump and nutrient upwelling are at least partly controlled by intermediate-deep water

50 circulation, contributing to the observed CO_2 changes (e.g., Toggweiler, 1999; Marchitto and Broecker, 2006).

51 To track past changes in the nutrient concentration of intermediate water masses, benthic foraminifera Cd/Ca has

52 been used in many recent studies (e.g., Came et al., 2008; Poggemann et al., 2017; Valley et al., 2017; Umling et

53 al., 2018); indeed, the benthic foraminifera Cd/Ca is a robust proxy of seawater cadmium concentrations (Cd_w)

54 (Boyle, 1988; 1992), which shows a positive linear correlation with labile nutrients (phosphate and nitrate) in the

55 modern ocean (e.g., Boyle et al., 1976; Boyle, 1988; Elderfield and Rickaby, 2000). The benthic foraminifera

56 incorporate Cd as a function of Cd_w with a species-dependent partition coefficient (e.g., Tachikawa and

57 Elderfield, 2002). Thus, the Cd measured in the fossil tests reflects the paleo-nutrient concentrations of the

58 surrounding water masses, and can be used to investigate past changes in intermediate-to-deep ocean properties

59 (e.g., Boyle and Keigwin, 1982; Oppo and Fairbanks, 1987; Came et al., 2008; Poggemann et al., 2017; Valley et

60 al., 2017; Umling et al., 2018).

61   Complementary to the geochemical proxies, the type of benthic foraminifers and their abundance, both of

62 which are related to organic flux and ecosystem oxygenation, make benthic foraminifer assemblages a powerful

63 proxy for estimating past variations in bottom water conditions (e.g., Corliss et al., 1986; Schmiedl et al., 1998;

64 Almogi-Labin et al., 2000) in conjunction with organic matter fluxes to the seafloor (e.g., Altenbach et al., 1999;

65 Van der Zwaan et al., 1999; Fontanier et al., 2002; Caulle et al., 2015). Benthic foraminifera have been

66 successfully used as indicators of surface productivity, especially in high carbon flux regions (Schnitker, 1994).

67 By comparing past benthic foraminiferal assemblages to modern ones, changes in food supply and oxygen

68 concentrations of the bottom water can be reconstructed (e.g., Corliss, 1979; Peterson, 1984; Murgese and De

69 Deckker, 2005). Recently, the combining of benthic foraminiferal assemblages and geochemical proxies has

70 received increasing attention and have been used to reconstruct the evolution of surface productivity and

71 upwelling intensity in the Indian Ocean (e.g., Hermelin 1991, 1992; Hermelin and Shimmield, 1995; Den Dulk

72 et al., 1998; Murgese and De Deckker, 2005).

73   The Arabian Sea is one of the most productive regions of the ocean today (Banse, 1987; Marra and Barber,

74 2005). Surface productivity is dominated by the monsoon system, which has a strong impact on the distribution

75 and dynamics of stratification and vertical mixing (Lévy et al., 2007). Numerous studies have focused on the

76 reconstruction of the paleo-productivity of the Arabian Sea in relation to past changes in monsoon intensity (e.g.,

77 Prell and Kutzbach, 1987; Naidu and Malmgren, 1996; Gupta et al., 2003; Singh et al., 2006; 2011; Bassinot et

78 al., 2011; Saraswat et al., 2014). By contrast, little is known about the paleoproductivity of the BoB, especially

79 its links to changes in monsoon precipitation (Phillips et al., 2014; Zhou et al., 2020). Consequently, studying

80 paleoproductivity and past nutrient concentration of intermediate water masses in the northeastern Indian Ocean

will also allow us to completely understand the influence of monsoon climate changes in tropical ocean ecology at different timescales. Besides, as the benthic foraminiferal Cd/Ca is a promising proxy to reconstruct the intermediate-deep water nutrient content (e.g., Boyle and Keigwin, 1982; Tachikawa and Elderfield, 2002; Came et al., 2008; Poggemann et al., 2017; Valley et al., 2017), most of the studies referred to above have reconstructed deep-intermediate water masses in the past (e.g., Came et al., 2008; Bryan and Marchitto, 2010; Poggemann et al., 2017; Valley et al., 2017), and only few works indicate the relationship between the intermediate water masses nutrient and surface productivity (Bostock et al., 2010; Olsen et al., 2016). Furthermore, the evolution of the nutrient content of intermediate water masses since the last deglaciation has never been reconstructed in the Indian Ocean, where only two low-resolution Cd/Ca records are available for deep-water depths (Boyle et al., 1995), and, to our knowledge, none are available for intermediate water depths.

In this study, we provide, for the first time, two benthic foraminifera Cd/Ca records at intermediate water depths in the northern Indian Ocean (Arabian Sea and northern Bay of Bengal). These data make it possible to estimate past changes in the nutrient content , since the last deglaciation, over the last 17 kyr BP. We have also investigated benthic foraminiferal assemblages obtained from core MD77-191 (southeastern Arabian Sea) to help us reconstructing the conditions at the seafloor. Combined with planktonic foraminiferal $\delta^{18}O$, benthic $\delta^{13}C$, and Cd/Ca records obtained from the same core, as well as with results already published in the Bay of Bengal (Ma et al., 2019; 2020), this study aims to document past variations in intermediate- and deep-water conditions and to decipher their links with surface paleo-productivity and intermediate water ventilation.

2. Material and modern hydrological setting

We analyzed sediment core MD77-191 (07°30'N-76°43'E, 1254m) located in the Arabian Sea (off the southern tip of India), and core MD77-176 (14°30'5N-93°07'6E, 1375m) retrieved in the northeastern Bay of Bengal (BoB). These cores were collected in 1977 during the OSIRIS III cruise of the French N/O Marion Dufresne (Fig. 1).

The age model of core MD77-191 was established by using accelerator mass spectrometry (AMS) ^{14}C dates obtained on 9 monospecific samples of planktonic foraminifera *Globigerinoides bulloides* (Bassinot et al., 2011), one sample of pteropods (Mléneck, 1997), and three samples of the planktonic foraminifera *Globigerinoides ruber* (Ma et al., 2020). The average sedimentation rate of core MD77-191 is about 53 cm./kyr[-1] and up to 90 cm/.kyr[-1] during the Holocene, providing a high-resolution, continuous record since 17 cal kyr BP.

The age model of core MD77-176 was previously established by using 31 planktonic foraminifer (*G. ruber*) AMS ^{14}C dates combined with the core MD77-176 oxygen isotope record obtained on planktonic foraminifera *G. ruber*, which were correlated to the GISP2 Greenland ice core record (Marzin et al., 2013). Core MD77-176 displays high accumulation rates (average ~25 cm.kyr[-1] and up to 40 cm.kyr[-1] during the Holocene).

In the modern ocean, the surface waters of the Arabian Sea and BoB are characterized by seasonally reversing currents that are driven by the monsoon winds (Fig1.a). The surface water masses shallower than 150 m in the Arabian Sea are mainly Arabian Sea high High Salinity Water (ASHS, 36.5 psu) (Talley et al., 2011). In the BoB, the surface waters above 100 m are designated Bay of Bengal surface waters (BoBSW), which have a low salinity (31 psu) due to large river inputs (Talley et al., 2011). Today, the northward extension of AAIW in the Indian Ocean rarely reaches beyond 10°S (Lynch-Stieglitz et al., 1994). The sites of cores MD77-191 and

121   MD77-176 are mainly bathed, therefore, by the North Indian Intermediate Water (Olson et al., 1993; Reid, 2003)

122   with a potential contribution from the Red Sea Outflow Water (RSOW) for the site MD77-191 (Beal et al., 2000).

123   Between 1500 and 3800m, the dominant deep water in the North Indian Ocean is Indian Deep Water (IDW),

124   originating from the Circumpolar Deep Water and North Atlantic Deep Water (NADW) ~~and from the southern~~

125   ~~return flow of deep water (North Indian Deep Water) for the site of core MD77-176~~ (Talley et al., 2011).

126   As far as surface waters are concerned, during the summer monsoon, the clockwise circulation in the

127   Arabian Sea drives high salinity waters from the northern to the southeastern Arabian Sea ~~(Fig. 1 and S1)~~. By

128   contrast, during the winter monsoon, the northeastern winds bring low salinity water (BoBSW) from the BoB.

129   The northern Indian Ocean, especially the Arabian Sea, is characterized by highly variable seasonal productivity

130   (Shankar et al., 2002). Southwest winds during the summer season induce a strong Ekman pumping resulting in

131   very active upwelling along the western coasts of the Arabian Sea and thus promoting strong surface

132   productivity (Shankar et al., 2002; Fig. S1). By contrast, the surface productivity in the BoB is generally weak

133   compared with the Arabian Sea (e.g., Prasanna Kumar et al., 2001; Thushara and Vinayachandran, 2016;

134   O'Malley, 2017; Fig. S1). In the BoB, large river inputs of fresh water and direct monsoon precipitation lead to

135   more stable stratification in the upper ocean (Vinayachandran et al., 2002), and hence the vertical mixing of

136   nutrients from the subsurface to the euphotic zone is generally limited (Gomes et al., 2000). However, the

137   primary productivity of the western BoB shows a slight increase during the winter monsoon, as indicated by the

138   distribution of chlorophyll in the surface water (Thushara and Vinayachandran, 2016; O'Malley, 2017; Fig. S1).

139   Modern data indicate that the southern-sourced intermediate water (AAIW) in the Indian Ocean has a

140   phosphate concentration of about 2-2.5 µmol/kg (Figs. 1b and c). In the Northern ~~intermediate~~ Intermediate

141   Indian Ocean, the phosphate concentration is significantly higher, ranging from 2.75 to 3 µmol/kg in the Arabian

142   Sea during the summer monsoon, and from 2.5 to 2.75 µmol/kg in the BoB during the winter monsoon (Figs. 1b

143   and c). The higher phosphate in the northern Indian Ocean can been linked to primary productivity (Banse, 1987;

144   Marra and Barber, 2005).

145

146   **3. Methods**

147   **3.1. Cd/Ca analysis**

148

149   In order to improve understanding of possible species level differences and microhabitat effects on the

150   benthic Cd/Ca records, w~~W~~e analyzed Cd/Ca in three calcite (*Cibicidoides pachyderma*, *Uvigerina peregrina*,

151   and *Globobulimina* spp.) and one aragonite (*Hoeglundina elegans*) benthic foraminiferal species from core

152   MD77-191. *C. pachyderma* is a~~n~~ shallow in~~epi~~faunal species, *U. peregrina* and *Globobulimina* spp. are

153   endobenthic species with intermediate and deep microhabitats, respectively (Fontanier et al., 2002). In core

154   MD77-176, due to the limitation of calcitic species, we only measured Cd/Ca ratios in *H. elegans* shells.

155   Each sample contained between 10 and 15 individuals picked from the 250-315µm size fraction. Samples

156   were gently crushed, cleaned to remove clays, organic matter and elemental oxides by using reductive and

157   oxidative cleaning following previously published methods (Boyle and Keigwin, 1982; Barker et al., 2003).

158   Each sample was dissolved in 0.075N HNO_3 and analyzed using a single collector sector field high resolution

159   inductively coupled plasma mass spectrometer (HR-ICP-MS) Thermo Element XR hosted at the GEOPS

160   Laboratory (University Paris-Saclay, France).

161   The detailed instrumental settings and mother standard solutions are described in Ma et al., (2020). A blank

consisting of the same 0.1N HNO_3 used to dilute the standards and samples was also analyzed. We removed the blank intensity values from all the raw intensities (including standards), and raw data were linearly drift-corrected by interspersing a drift standard every four samples. Standard curves were used to calculate elemental concentrations, coefficients of determination (r^2) always being >0.9999 for all elemental ratios. The mean reproducibility and accuracy are 3.6% and 7.5%, respectively.

3.2 Faunal analysis

Benthic foraminiferal assemblages from core MD77-176 have already been published in Ma et al. (2019). For core MD77-191, a total of 72 samples were collected for benthic foraminiferal assemblage determinations. In each sample, benthic foraminifera (>150-μm) were extracted, counted and identified to species level following the taxonomical descriptions of various authors (e.g., Loeblich and Tappan, 1988; Jones, 1994; Holbourn et al., 2013). For core MD77-191, there is no material left in this old, low diameter core and so we used samples obtained earlier for stable isotope studies. Since the bulk weights of these samples were not recorded prior to sieving, we could not perform the calculation of absolute abundance of foraminifera or accumulation rates. Thus, we only converted the individual counts to percentages with respect to the total benthic foraminifera present in each sample. In order to describe major faunal variations, we performed principal component analysis (PCA) on the variance-covariance matrix using the PAST software (Version 3.0, Hammer et al., 2001). Species present with a percentage >1% in at least 1 sample were used for statistical analysis and diversity calculation.

4. Results

4.1. Elemental ratios results

To check the influence of oxide contaminants on the elemental ratios, Mn/Ca was systematically measured. The Mn/Ca of *H. elegans* from cores MD77-191 and MD77-176 ranges between 6.5-10 μmol/mol and 1-30 μmol/mol, respectively. Such ranges are much lower than the 100 μmol/mol limit proposed by Boyle (1983). The Mn/Ca obtained on the three calcite benthic foraminifera species from core MD77-191 - *C. pachyderma* (5-18 μmol/mol), *U. peregrina* (3-23 μmol/mol) and *Globobulimina* spp. (4-69 μmol/mol) - are also all below 100 μmol/mol (Boyle, 1983). The Fe/Ca ratios are also lower than 1 mmol/mol in all samples from cores MD77-191 and MD77-176, in agreement with the limit proposed by Barker et al. (2003). In addition, Barker et al. (2003) concluded that no significant pollution by clay minerals would be expected when Al/Ca is <0.5 mmol/mol. In all our samples, Al/Ca is below 0.5 mmol/mol, indicating that the sample cleaning procedure was efficient.

All of the above results indicate that our samples were not affected by contamination.

4.1.1 Cd/Ca

The Cd/Ca records of *C. pachyderma*, *U. peregrina* and *Globobulimina* spp. from core MD77-191 range between 0.07-0.2 μmol/mol, 0.07-0.14 μmol/mol and 0.03-0.09 μmol/mol, respectively (Figs. 2e gd; supplementary Table S1).

The Cd/Ca records for the calcite benthic species *C. pachyderma* and *U. peregrina* have very low time resolutions during the last deglaciation. However, some common patterns can be observed. The Cd/Ca records of *C. pachyderma* and *U. peregrina* show lower values during the Heinrich stadial 1 (HS1, 17-15.2 cal kyr BP) and

Younger Dryas (YD, ~~12~~13-11 cal kyr BP) cold periods, with average values of ~0.08 μmol/mol for *C. pachyderma* and ~0.09 μmol/mol for *U. peregrina*. By contrast, these two species display higher Cd/Ca ratios (~0.12 μmol/mol) during the Bølling-Allerød warm period (B-A, 15-13.3 cal kyr BP) compared with the HS1 and YD. Then, lower values (~0.1 μmol/mol for *C. pachyderma*; 0.11 μmol/mol for *U. peregrina*) are observed during the early Holocene (10-5 cal kyr BP) compared to larger variations occurring in the late Holocene (5.2-2.4 cal kyr BP). The Cd/Ca record of deep infaunal *Globobulimina* spp., obtained at a lower time resolution, shows different variations compared with the two other taxa without any clear trend during the Holocene.

The *H. elegans* Cd/Ca values of core MD77-191 range from 0.05 to 0.31μmol/mol since 17 cal kyr BP (Fig. 2d; supplementary Table S1). Depleted values at about 0.07 μmol/mol are recorded from the last deglaciation to the early Holocene (17-5 cal kyr BP time interval). During the HS1 and the YD time intervals ~~over the last deglaciation~~, a significant decrease of about ~0.~~05~~06 μmol/mol occurred (even when taking into consideration the analytical error bar of ±0.02, 2σ), and a slight increase (0.09 μmol/mol) is observed between 15 and 13.3 cal kyr BP (B-A period). A rapid increase in the Cd/Ca values beginning at 5.2 cal kyr BP reaches a maximum (0.31 μmol/mol) during the late Holocene.

For core MD77-176, the *H. elegans* Cd/Ca records range between 0.06 and 0.17 μmol/mol over the past 18 cal kyr BP (Fig. 2e~~h~~; supplementary Table S1), without no clear trends and average benthic Cd/Ca values of ~0.09 μmol/mol during the different periods (HS1, YD and Holocene). However, the benthic Cd/Ca record during the Holocene seems to exhibit a slight increase both in value and range of variations after 6 cal kyr BP.

4.2. Foraminifera assemblages of core MD77-191

Benthic foraminiferal species richness ranges between 16 and 36, and the total abundance fluctuates between 82 and 642 specimens (supplementary Table S2). Hyaline species are the dominant constituents (＞80%), and mainly consist of *Bulimina aculeata*, *H. elegans*, *C. pachyderma*, *Uvigerina* spp., *Gyroidina broeckhiana*, *Globocassidulina subglobosa*, *Sphaeroidina bulloides*, *Gyroidinoides* spp., *Lenticulina* spp., *Melonis barleeanum*, and *Globobulimina* spp. (including *Praeglobobulimina* spp.) (in decreasing order of relative average abundance). Agglutinated taxa reach on average about 1.6%, and consist of *Textularia* sp., *Martinottiella communis,* and *Eggerella bradyi*. The average percentage of porcelaneous species, characterized by *Pyrgo elongata*, *Pyrgo murrhina*, *Pyrgo depressa*, *Pyrgoella irregularis*, *Quinqueloculina* spp., *Sigmoilopsis schlumbergeri*, and *Spiroloculina* spp., is about 5.1%.

Furthermore, we merged species that share an ecological similarity, such as *Globobulimina affinis*, *Globobulimina pacifica*, and *Praeglobobulimina* spp. into *Globobulimina* spp. A total of 74 samples and 55 groups/species were adopted to perform principal component analysis (PCA) in order to identify major faunal trends. The PCA analysis suggests that the benthic foraminifera could be grouped into three assemblages, and represent about 61% of the total variance (Table 1).

The combination of *Bulimina aculeata* and *C. pachyderma*, together with *Pullenia bulloides* and *Ehrenbergina trigona* (Figs. 3 and S2), display high positive PC1 loadings. This assemblage, referred hereafter as assemblage 1, dominated the foraminiferal record during the late Holocene (between 6 and 1.4 cal kyr BP). By contrast, *H. elegans* and *Bulimina manginata* exhibit high negative PC1 loadings, and dominate assemblage 2,

which corresponds to the record during the early Holocene (Figs. 3 and S2). Other quantitatively important contributors are *C. wuellerstorfi* and *Globocassidulina subglobosa* (Fig. S2).

The total variance of PC2 is 19%; for the positive loadings of PC2, *Sphaeroidina bulloides* and *Gyroidinoides orbicularis* dominate assemblage 3, which is more important during the last deglaciation (Figs. 3 and S2). The main associated species of assemblage 3 are *Bulimina mexicana* and *Gyroidinoides soldanii* (Fig. S2). However, the main species from negative loadings consist of *Bulimina aculeata*, *H. elegans* and *C. pachyderma*, which dominated the Holocene. The main composition of PC2 negative loadings is dominated by the same benthic species as assemblages 1 and 2, which, as we have seen above, correspond to the Holocene; it is difficult, therefore, to glean any additional information from this regarding bottom conditions. For this reason we only recognize three assemblages in this paper.

5. Discussion

5.1. Past intermediate water Cd_w concentrations from the Northern Indian Ocean

In the modern ocean, benthic foraminifera Cd/Ca shows a positive correlation with Cd_w and dissolved nutrients (phosphate and nitrate) (Boyle et al., 1976; Hester and Boyle, 1982). As aragonitic~~aragonite~~ benthic foraminifera *H. elegans* faithfully records the bottom water Cd concentrations (Cd_w), Cd/Ca ratios can be converted to seawater Cd_w with the appropriate relationship (Eq.1), where the partition coefficient $D_p \approx 1$ for all water depths (Boyle et al., 1995; Bryan and Marchitto, 2010).

$$Dp = \frac{(Cd/Ca)_{foram}}{(Cd/Ca)_{water}} \qquad \text{(Eq.1)}$$

In contrast, the partition coefficient for calcite species changes with water depth. For water depths between 1150-3000 m, D_p was calculated based on the equation of Boyle, (1992; Eq. 2). The seawater Ca concentration is assumed to be at a constant, mean value of 0.01 mol/kg (Boyle, 1992).

$$D_p = 1.3 + (\text{depth} - 1150) \times (1.6/1850) \qquad \text{(Eq.2)}$$

The intermediate Cd_w results based on the *H. elegans* Cd/Ca values of core MD77-191, range from 0.5 to 3.1 nmol/kg since 17 cal kyr BP (Fig. 4a), with a core top value of 0.80 nmol/kg in agreement with the estimated intermediate water depth modern Cd_w (~0.83 nmol/kg) in the northern Indian Ocean (Boyle et al., 1995). The intermediate Cd_w was also calculated from calcite benthic species *C. pachyderma, U. peregrina* and *Globobulimina* spp. from core MD77-191, with values ranging between 0.53-1.48 μmol/mol, 0.52-1.04 μmol/mol and 0.26-0.65 μmol/mol, respectively (Fig. 4a). The Cd_w values of *C. pachyderma* and *U. peregrina* are within the same range. However, the *H. elegans* Cd_w values are higher than those from the two calcite species, especially during the Late Holocene. Moreover, the core top data of *C. pachyderma* and *U. peregrina* are also lower (~ 0.7 and 0.69 nmol/kg, respectively) than the modern estimated Cd_w data (~ 0.83 nmol/kg) in the northern Indian Ocean (Boyle et al., 1995) (Fig. 4a). These depleted Cd_w values may be related to the benthic foraminiferal microhabitat effect; indeed, *U. peregrina* is known to be strictly a shallow infaunal species, as well

283 as *C. pachyderma* (Fontanier et al., 2002), differing from strictly epifaunal taxa, such as *Cibicidoides*

284 *wuellerstorfi* (Mackensen et al., 1993).

285 Besides, the deep infaunal *Globobulimina* spp. Cd_w displays relatively much lower values and does not

286 exhibit strong variations compared to the other species investigated in this study, displaying a general increasing

287 trend from the last deglaciation to the Holocene. As *Globobulimina* spp. correspond to deep benthic infaunal

288 species, this result may indicate a stable nutrient content of pore water, as compared to other benthic taxa

289 associated with bottom water (Fig. 4a). Thus, when tracking past changes in the bottom water Cd_w

290 concentrations, the use of a strictly epifaunal species living at the water-sediment interface such as *H. elegans*

291 appears to be more robust than using endofaunal species that live in contact with pore water.

292 Relative variations in the Cd_w obtained from *C. pachyderma* and *U. peregrina* are in good agreement with the

293 records obtained on *H. elegans.* Variations of *H. elegans* Cd_w during the last deglaciation indicate a decrease of

294 about ~0.5–6 nmol/kg in the HS1 and YD periods, with a slight increase (0.9 nmol/kg) during the warm B-A.

295 Cd_w results from core MD77-191 indicate a shift from the last deglaciation (~0.8–7 nmol/kg) to the late Holocene

296 (~1.59 nmol/kg). During the Holocene, the Cd_w records display relatively low values of around 0.9 nmol/kg in

297 the 10-6 cal kyr BP time interval, and show a major shift at around 6.4 cal kyr BP with values rising up to 3.1

298 nmol/kg.

299 ~~The intermediate Cd_w was also calculated from calcite benthic species *C. pachyderma*, *U. peregrina* and~~

300 ~~*Globobulimina* spp. from core MD77-191, with values ranging between 0.53-1.48 µmol/mol, 0.52-1.04~~

301 ~~µmol/mol and 0.26-0.65 µmol/mol, respectively (Figs. 4b-d). The Cd_w values of *C. pachyderma* and *U.*~~

302 ~~*peregrina* are within the same range. However, the deep infaunal *Globobulimina* spp. Cd_w displays relatively~~

303 ~~much lower values and does not exhibit strong variations compared to the other species investigated in this study,~~

304 ~~displaying a general increasing trend from the last deglaciation to the Holocene. As *Globobulimina* spp.~~

305 ~~correspond to deep benthic infaunal species, this result may indicate a stable nutrient content of pore water, as~~

306 ~~compared to other benthic taxa associated with bottom water (Fig. 4d).~~

307 ~~During the last deglaciation, the Cd_w records of *C. pachyderma* and *U. peregrina* show a decreasing trend~~

308 ~~during the HS1 and YD events, with mean values of ~ 0.59 and 0.65 nmol/kg for *C. pachyderma* and ~ 0.62 and~~

309 ~~0.67 nmol/kg for *U. peregrina*, respectively (Fig. 4b and c). The Cd_w records all display higher values during the~~

310 ~~B-A, with average values of ~ 0.94 and 0.84 nmol/kg, respectively (Fig. 4b and c). The Cd_w records show~~

311 ~~depleted values in the early Holocene, followed by an abrupt increase during the middle Holocene, with average~~

312 ~~values of ~0.87 nmol/mol for *C. pachyderma* and ~0.81 nmol/kg for *U. peregrina*.~~

313 ~~Relative variations in the Cd_w obtained from *C. pachyderma* and *U. peregrina* are in good agreement with the~~

314 ~~records obtained on *H. elegans*. However, the *H. elegans* Cd_w values are higher than those from the two calcite~~

315 ~~species, especially during the Late Holocene. Moreover, the core top data of *C. pachyderma* and *U. peregrina*~~

316 ~~are also lower (~ 0.70 and 0.69 nmol/kg, respectively) than the modern estimated Cd_w data (~ 0.83 nmol/kg) in~~

317 ~~the northern Indian Ocean (Boyle et al., 1995). These depleted Cd_w values may be related to the benthic~~

318 ~~foraminiferal microhabitat effect; indeed, *U. peregrina* is known to be strictly a shallow infaunal species, as well~~

319 ~~as *C. pachyderma* (Fontanier et al., 2002), differing from strictly epifaunal taxa, such as *Cibicides wuellerstorfi*~~

320 ~~(Mackensen et al., 1993). Thus, when tracking past changes in the bottom water Cd_w concentrations, the use of a~~

321 ~~strictly epifaunal species living at the water-sediment interface such as *H. elegans* appears to be more robust than~~

322 ~~using endofaunal species that live in contact with pore water.~~

323   For core MD77-176, the intermediate water Cd_w calculated from the *H. elegans* Cd/Ca records ranges between
324   0.6 and 1.7 nmol/kg over the past 18 cal kyr BP (Fig. ~~4e~~4b). Compared with intermediate Cd_w from MD77-191,
325   the Cd_w record of core MD77-176 does not display any clear trend from the last deglaciation to the Holocene.
326   However, a slight increase is observed since 6 cal kyr BP, in agreement with the MD77-191 intermediate Cd_w
327   records. In addition, even though the MD77-176 record has a lower time resolution, it displays a shorter
328   maximum (1.3 nmol/kg) during the 13.4-11 cal kyr BP time interval.

329   To summarize, among the three calcite benthic taxa and the aragonitic benthic species *H. elegans*, the Cd/Ca
330   records of *H. elegans* appear to be the most suitable for tracking past Cd_w changes at intermediate water depth
331   through time. Thus, in the following discussion, we will only focus on the intermediate Cd_w calculated from the
332   *H. elegans* Cd/Ca from both studied cores.

333

334   **5.2. Comparison between geochemical records and benthic foraminiferal assemblages**
335

336   Comparing the geochemical records to the benthic assemblages, we can observe similar patterns. For core
337   MD77-191 from the southeastern Arabian Sea, three benthic assemblages were identified since the last
338   deglaciation. *S. bulloides* and *Gyroidinoides orbicularis* are major components of assemblage 3 (during the last
339   deglaciation), together with *B. mexicana* and *Gyroidinoides soldanii* (Figs. 3 and S2). *S. bulloides* and *B.*
340   *mexicana* are found in intermediate to high organic carbon flux rate regions (e.g., Schmiedl et al., 2000;
341   Eberwein and Mackensen, 2006, 2008), while *G. orbicularis* and *G. soldanii* are associated with well-
342   oxygenated and oligotrophic environments (Peterson, 1984; Burmistrova and Belyaeva, 2006; De and Gupta,
343   2010). Thus, assemblage 3 reflects mesotrophic environments and/or well-ventilated conditions during the last
344   deglaciation. Although millennial-scale changes in the benthic foraminiferal assemblages during the last
345   deglaciation could not be observed, benthic fauna 3 seems at least partly consistent with previous studies in the
346   northern Indian Ocean based on multiple geochemical proxies (e.g., benthic $\delta^{13}C$, intermediate water $[CO_3^{2-}]$ and
347   ε_{Nd} records); these studies have revealed the presence of better-ventilated waters, which might correspond to
348   AAIW, during the HS1 and YD (e.g., Yu et al., 2018; Ma et al., 2019; 2020).

349   Benthic foraminiferal assemblage 2 predominates during the early Holocene and is characterized by *H.*
350   *elegans* and *B. manginata* as major contributors (Figs. 3 and S2). The other important contributors are *C.*
351   *wuellerstorfi* and *G. subglobosa*. *B. manginata* is found in high organic carbon flux rate conditions (De Rijk et
352   al., 2000; Eberwein and Mackensen, 2006, 2008). However, previous studies on *H. elegans*, *C. wuellerstorfi* and
353   *G. subglobsa* indicate that these species correspond to high levels of dissolved oxygen and oligotrophic settings
354   (e.g., Altenbach et al., 1999; Fontanier et al., 2002; Murgese and De Deckker, 2005, 2007; De and Gupta, 2010).
355   Periods dominated by these taxa probably indicate high oxygen levels and an oligotrophic environment.
356   Additionally, glacial to Holocene benthic $\delta^{13}C$ shifts (0.35-0.4‰, vs. PDB) at intermediate-deep water depth in
357   the northern Indian Ocean are interpreted as reflecting an increased contribution of better-ventilated deep water~~,~~
358   ~~namely North Atlantic Deep Water (~~NADW~~)~~, during the Holocene (e.g., Naqvi et al., 1994; Ma et al., 2019) (Fig.
359   S3). Futhermore, the increased B-P age offsets and depleted ε_{Nd} records obtained from the same core site could
360   reflect the enhanced influence of NADW during the Holocene, which is characterized by the well-ventilated and
361   depleted nutrient (modern Cd_w, ～0.2 nmol/kg) (Poggemann et al., 2017; Yu et al., 2018; Ma et al., 2019).

362   Although the intermediate benthic $\delta^{13}C$ record from core MD77-191 is missing for the LGM, the average value

for the Holocene (~0.31‰, vs. PDB) is consistent with previous studies carried out in the northern Indian Ocean:, combined with the opposite trend between $\delta^{18}O_{ivc}$ records and intermediate water temperature from MD77-191 (Ma et al., 2020), all these records and may also be associated suggest with well-ventilated conditions (Fig. S3). The predominance of Benthic foraminifera assemblage 2 in the early Holocene seems be in agreement with the higher values of benthic $\delta^{13}C$, reflecting better-ventilated water masses, associated with NADW, at the core site.

By contrast, *B. aculeata* and *C. pachyderma* are major components of assemblage 1 (during the late Holocene), together with *P. bulloides* and *E. trigona* (Figs. 3 and S2). Living *B. aculeata* have a widespread distribution, with a preference for water depths ranging from 1500 to 2500m, and are typically associated with high organic carbon fluxes (Mackensen et al., 1995; Almogi-Labin et al., 2000; Caulle et al., 2015). *P. bulloides* is a shallow infaunal species, which prefers mesotrophic environments and shows adaptability with respect to oxygen concentration in the Arabian Sea (Gupta and Thomas, 1999; Caulle et al., 2015). *E. trigona* is commonly recorded in low oxygen habitats (Caulle et al., 2015). We thus interpret assemblage 1 as indicating relatively low-oxygen and meso- to eutrophic bottom water conditions during the late Holocene (6-1.4 cal kyr BP). However, the lower oxygen concentrations reflected by benthic fauna 1 seem to be the opposite of what would be expected under an enhanced influence of better ventilated NADW during the Holocene in the northern Indian Ocean. The higher relative abundances of *Globigerina bulloides*, a proxy of upwelling activity, observed in the late Holocene of the same core, MD77-191, suggest increased productivity in the southeastern Arabian Sea (Bassinot et al., 2011) (Fig. 5). This record is synchronous with the benthic foraminiferal assemblage 1 (during the late Holocene). Thus, increased surface productivity during the late Holocene could result in more organic matter in the bottom water, leading to depleted oxygen conditions in bottom water.

When we compare benthic assemblages 2 and 3 (during the last deglaciation and early Holocene; 17-6 cal kyr BP) to the Assemblagefauna 1 (during the late Holocene), assemblages 2 and 3 indicate that intermediate water masses were characterized by higher bottom water oxygen conditions and a lower flux of organic matter. This is associated with depletedlow *Globigerina bulloides* abundances during the same time interval compared with the late Holocene, suggesting lower productivity in the southeastern Arabian Sea in the period from the last deglaciation to the Holocene (Bassinot et al., 2011) (Fig. 5). Therefore, all of these elements suggest that changes in primary productivity seem to be the main factor impacting on the distribution of benthic assemblages at core MD77-191 site, especially during the Holocene, rather than changes in intermediate-water circulation.

In addition, the total organic carbon (C_{org}) could also be used as a qualitative indicator of past productivity and/or bottom water ventilation changes (Naidu et al., 1992; Canfield, 1994; Calvert et al., 1995; Naik et al., 2017). In order to examine the relationships between intermediate Cd_w and these different processes (surface productivity and/or water mass ventilation) since the last deglaciation in the eastern Arabian Sea, we compared the MD77-191 Cd_w values with the relative abundance of *G. bulloides* and benthic foraminiferal assemblage analyses from the same core MD77-191, together with the records for C_{org} and the *G. bulloides* percentage obtained from core SK237 GC04 (1245m, southeastern Arabian Sea, Naik et al., 2017) (Fig. 5). Despite a lower resolution for The MD77-191 *H. elegans* Cd_w records, when compared to the C_{org} and the *G. bulloides* percentage from core SK237 GC04, all of them seem to exhibit similar trends at the long-time scale from the last deglaciation to Holocene; however, some little discrepancies can be observed at millennial time scales, especially during the late Holocene display a strong co-variation with the C_{org} from core SK237 GC04 since 17 cal kyr BP, and are also in good agreement with the relative abundance of *G. bulloides* records during the

Holocene (Fig. 5). In addition, the Cd_w records display a significant shift from the last deglaciation (~ 0.5 nmol/kg) to the late Holocene (~1.59 nmol/kg), and the intermediate Cd_w values are extremely high during the late Holocene. As mentioned before, increased influence of NADW was observed during the Holocene in the northern Indian Ocean (Yu et al., 2018; Ma et al., 2019; 2020). However, NADW is characterized by the depleted nutrient content (modern Cd_w, $\sim$0.2 nmol/kg; Poggemann et al., 2017), and thus this should indicate that deep-intermediate water masses variations does not seem to play an important role during the Holocene in this area. Besides, previous studies have suggested that increased Cd_w values (>1 nmol/kg) could correspond to elevated surface productivity (Bostock et al., 2010; Olsen et al., 2016). Thus, we suggest the intermediate Cd_w at core MD77-191 site was may be mainly influenced by surface productivity, especially during the Holocene.

Compared with benthic foraminifera fauna analysis from MD77-191 in the Arabian Sea (Figs. 3 and S2), the benthic assemblages of core MD77-176 suggest that the intermediate water masses were characterized by oligotrophic to mesotrophic conditions and/or well-ventilated environments during the Holocene (Ma et al., 2019), associated with much lower surface productivity (Fig. S4). This observation is in agreement with low primary productivity during the Holocene reconstructed by the relative abundance of coccolith species *Florisphaera profunda* from the same core MD77-176 in the northeastern BoB (Zhou et al., 2020). In the modern ocean, Prasanna Kumar et al. (2001) indicate that primary productivity in the BoB is much lower than in the Arabian Sea, the lower surface productivity resulting from the large freshwater input from river and direct rainfall as a result ofresulting from enhanced Indian Summer Monsoon precipitation (e.g., Vinayachandran et al., 2002; Madhupratap et al., 2003; Gauns et al., 2005). Moreover, when we compare the average Cd_w value of core MD77-176 from the BoB (~0.9 nmol/kg) with results from core MD77-191 in the Arabian Sea (~1.2 nmol/kg), lower values, especially during the late Holocene, are in agreement with the benthic assemblages.

To sum up, variations in the benthic assemblages seem to be associated with changes in the organic matter flux, linked to surface productivity, especially in the Arabian Sea (Schnitker, 1994). The benthic foraminiferal fauna are consistent with the Cd_w record of core MD77-191 particularly during the late Holocene (6-1.4 cal kyr BP). Thus, our results seem to show that the Cd_w record of Cd_w is mainly controlled by changes occurring at the surface, especially during the Holocene. However, at millennial time scales, such during the HS1 and YD, the percentages of planktonic species *G. bulloides* from cores MD77-191 and SK237 GC04 all indicate a slight increase inmodest paleo-productivity, the opposite of what is suggested by the results of core MD77-191 Cd_w and C_{org} obtained from core SK237 GC04. This interval is also marked by enriched *G. ruber* δ^{18}O values, indicating a weaker monsoon and reduced freshwater inputs (Naik et al., 2017). This apparent discrepancy may be related to changes in the intermediate water mass sources and/or ventilation during the last deglaciation. Therefore, we will discuss these issues in greater detail below in order to decipher these different processes.

5.3. Relationships between primary productivity and monsoon intensity

During the Holocene, the intermediate Cd_w records obtained from cores MD77-191 and MD77-176 display depleted values in the early Holocene, followed by an abrupt increasing trend at the middle Holocene, and then reach a maximum during the late Holoceneshow a decreasing trend between 5.2 and 2.4 cal kyr BP.

Of the two cores, core MD77-176, located in the northeastern BoB, shows the lowest intermediate Cd_w (down to ~ 0.83 nmol/kg) during the 10-6 cal kyr BP time interval. Observations described above suggest that this low

443   in Cd_w resulted from low primary productivity and thus reduced fluxes of organic matter to the intermediate

444   depths. We attribute this evolution to monsoon variation. The early Holocene Climate Optimum (10-6 cal kyr BP)

445   is characterized by enhanced monsoon precipitation (Marzin et al., 2013; Contreras-Rosales et al., 2014) (Figs.

446   6c d-fe) that resulted in increased freshwater discharge from the Ganges-Brahmaputra river system and from the

447   Irrawaddy River. However, the distribution of chlorophyll in surface water of the western BoB suggests a low

448   annual productivity, indicating that the BoB is not significantly influenced by the riverine nutrient input (Zhou et

449   al., 2020). Thus, iIt is likely that this increase in fresh water drove pronounced ocean stratification in the

450   northeast BoB, which could impede the nutrient transfer from deep layer to the euphotic upper seawater column,

451   and then inducing low productivity.

452   A similar low in Cd_w is observed in the reconstructed intermediate water Cd_w record from core MD77-191

453   during the early Holocene, with values descending to ~ 0.92 nmol/kg, in the 10-6 cal kyr BP time interval. These

454   low values of intermediate Cd_w are coeval with low surface productivity as recorded by the *G. bulloides*

455   percentage and low values in C_{org} content from SK237 GC04 in the Arabian Sea. Off the southern tip of India,

456   we cannot reject the possibility that increased monsoon precipitation and enhanced freshwater runoffs in the BoB

457   during the early Holocene, inducing a stronger stratification, could explain part of the decrease in surface

458   primary productivity. Yet, at this site, another explanation prevails which is related to the decrease of summer

459   monsoon wind intensity that drives local Eekman pumping. As shown by Bassinot et al. (2011), the productivity

460   variations at the southern tip of India are inversely related to the evolution of upwelling activity along the Oman

461   Margin, to the west of the Arabian Sea. Based on a data/model comparison, Bassinot et al. (2011) showed that

462   this anti-correlation can be attributed to the northward shift of the ITCZ when boreal summer insolation reached

463   a maximum in the early Holocene (Fig. 6a); this ITCZ location results in enhanced summer monsoon wind

464   intensity and an increase in the associated Eekman pumping in the west of the Arabian Sea, and along the Oman

465   margin, while it weakens at the southern tip of India. This process may thus induce a decrease in surface

466   productivity in the southeastern Arabian Sea.

467   In addition, Naik et al. (2017) pointed out the co-existence of low productivity during the early Holocene in

468   the BoB and to the South of India, in agreement with our data that clearly show the impact of such a reduction of

469   surface primary productivity on the intermediate water Cd_w. These authors suggested a direct relationship

470   between intense monsoon rainfall and reduced surface productivity. However, the northeastern BoB received a

471   much larger amount of river input than the southern tip of India during the early Holocene (Marzin et al., 2013).

472   Thus, it seems reasonable to propose that the northeastern BoB is more affected by the salinity-related

473   stratification effect, while the southern tip of India is more affected by the decrease in wind intensity (Bassinot et

474   al., 2011) with enhanced stratification being potentially made stronger by an additional fresh-water effect,

475   although weaker than in the BoB. Ultimately, both climatic features (summer wind intensity and precipitation)

476   are directly under the control of monsoon evolution resulting from the orbital forcing of low latitude boreal

477   summer insolation.

478   By contrast, higher intermediate Cd_w values from core MD77-191 associated with higher *G. bulloides* relative

479   abundances and C_{org} from core SK237 GC04 during the 5.2-2.4 cal kyr BP time interval could indicate enhanced

480   productivity during the mid to late Holocene (Naik et al., 2017) (Fig. 5). To a lesser extent, this is also observed

481   in the records from the Northern BoB for the same time-period. These changes are consistent with a the

482   weakened summer monsoon intensity, with less rainfall during the late Holocene, as observed in the BoB using

core MD77-176 seawater $\delta^{18}O$ and core SO188-342KL δD_{Alk-ic} records (Marzin et al., 2013; Contreras-Rosales et al., 2014; Figs. 6e-f). ~~and~~ In addition, this is also strongly supported by the $\delta^{13}C_{wax}$ records from the Lonar Lake over the Indian continent ~~(Marzin et al., 2013; Contreras-Rosales et al., 2014;~~ (Sarkar et al., 2015; Fig. 6d)~~,~~ and a progressive increase in monsoon summer winds to the South of India (Bassinot et al., 2011) ~~(Fig. 6)~~. These observations could also strongly support the hypothesis that the major control on surface productivity is linked to monsoon evolution in the BoB and at the southern tip of the Arabian Sea during the Holocene (Bassinot et al., 2011; Naik et al., 2017; Zhou et al., 2020).

5.4. Millennial-scale changes in intermediate water circulation during the deglaciation

During the last deglaciation, short events have been recorded at the site of core MD77-191 during the 16-15.2 (HS1) and 12.6-11 cal kyr BP (YD) time intervals (Fig. 5). The low Cd_w values in the MD77-191 record are coeval with reductions of C_{org} in core SK237 GC04 during the HS1 and YD periods (Fig. 5). According to previous studies, extremely high Cd_w values (>1 nmol/kg) were reported to have been associated with enhanced surface productivity (Bostock et al., 2010; Olsen et al., 2016). However, the range of values of intermediate Cd_w (0.58-0.85 nmol/kg, HS1; 0.5-0.8 nmol/kg, YD) from core MD77-191 during the last deglaciation is much lower compared with the Holocene Cd_w values (>1 nmol/kg), and thus may be associated with other processes such as a better ventilation, changes in the water mass source, and/or depleted surface productivity (Fig. ~~7~~6). Significant decreases in *G. bulloides* relative abundance of cores SK237 GC04 (Naik et al., 2017) and MD77-191 records were observed from the HS1 to B-A (Bassinot et al., 2011) ~~(Fig. 5).~~, and thereafter slight increases occurred in the YD (Fig. 5). ~~Although a slight increase occurred in the YD, the *G. bulloides* percentage records from both cores show a general depletion during the last deglaciation compared with the last glacial interval and late Holocene (Fig. 5). Thus, we do not expect that surface productivity played an important role during the last deglaciation. In addition, compared with the relative percentage of *G. bulloides* during the B-A, slightly~~ These high~~er~~ values at both core sites during the HS1 and YD may indicate an ~~small, but net~~ enhanced~~increase of~~ surface productivity during these intervals (Fig. 5). This should have led to increased intermediate Cd_w and organic matter preservation under ~~conditions of~~ low oxygen concentration conditions during the HS1 and YD. However, despite a low resolution for the MD77-191 Cd_w record during the last deglaciation, ~~But,~~ we do not observe ~~a decrease~~high values of intermediate Cd_w during the HS1 and YD ($\sim$0.6 nmol/kg) compared with the late Holocene (~1.59 nmol/kg), ~~in these two proxies~~ especially at 16.5-16 cal kyr BP~~,~~. ~~the opposite of what would be expected from stronger surface productivity. Thus,~~ Although we cannot fully discard the influence of surface productivity on the intermediate Cd_w in these time intervals, this apparent discrepancy seems to provide~~s~~ another evidence for the influence of changes in water masses and/or ventilation during the HS1 and YD, as already demonstrated by previous studies and proxies in the northern Indian Ocean (Bryan et al., 2010; Yu et al., 2018; Ma et al., 2019; 2020).

Moreover, an increase in benthic $\delta^{13}C$ values is observed during the HS1 and YD in the northern Indian Ocean (e.g., Duplessy et al., 1984; Curry et al., 1988; Naqvi et al., 1994; Jung et al., 2009; Ma et al., 2019). The increase in the different benthic $\delta^{13}C$ records during the HS1 and YD in the western Arabian Sea, Pacific Ocean and BoB is interpreted as reflecting the northward expansion of AAIW (Pahnke and Zahn, 2005; Jung et al., 2009; Ma et al., 2019). The decreased benthic-planktonic foraminiferal ^{14}C offset (B-P age) obtained from

523 marine sediment cores from the Arabian Sea and the Bay of Bengal during the same intervals could confirm
524 enhanced vertical mixing in the Southern Ocean (Bryan et al., 2010; Ma et al., 2019). The transition in the ε_{Nd}
525 and $\Delta^{14}C$ records during the deglaciation also indicates a strong northward penetration of AAIW within the
526 North Atlantic and Bay of Bengal (e.g., Cao et al., 2007; Pahnke et al., 2008; Pena et al., 2013; Yu et al., 2018).
527 In addition, during the HS1 and YD, a decrease in the $[CO_3^{2-}]$ record from core MD77-191 also suggests the
528 release of CO_2 from the deep ocean in the deglacial period through the expansion of AAIW (Ma et al., 2020).
529 These time intervals are associated with better ventilation in the Southern Ocean (e.g., Anderson et al., 2009;
530 Skinner et al., 2010), which led to enhanced vertical ventilation resulting in increased production of intermediate
531 water masses (AAIW) (Anderson et al., 2009).

532   As mentioned before, previous studies have suggested an enhanced northward flow of southern sourced
533 intermediate water mass AAIW both in the Atlantic, Pacific and Indian Oceans during the last deglaciation (e.g.,
534 Pahnke et al., 2008; Bryan et al., 2010; Poggemann et al., 2017; Yu et al., 2018; Ma et al., 2019, 2020),
535 indicating that the source of intermediate water masses may be partly the same in these oceans. Thus, ~~by using~~ as
536 the benthic $\delta^{13}C$ values collected from the north Indian Ocean could~~to~~ better constrain the influence of AAIW in
537 the two studied cores (Naqvi et al., 1994; Jung et al., 2009; Ma et al, 2019; 2020), we can also compare the range
538 values of AAIW Cd_w ~~obtained~~ from ~~the~~ both studied cores ~~MD77-191 and MD77-176~~ with ~~other oceans,~~
539 ~~including~~ data from ~~the~~ Atlantic and Pacific Oceans at intermediate water depth during the HS1 and YD (Cd_w,
540 0.3-0.9 nmol/kg; Umling et al., 2018; Valley et al., 2017). Unfortunately, the resolution of both intermediate Cd_w
541 and benthic $\delta^{13}C$ from core MD77-176 (northeastern BoB) are very low for the HS1 and YD events, making it
542 difficult to extract reliable information. Thus, we have decided to focus on the results from core MD77-191 (0.5-
543 0.85 nmol/kg) during these two time-intervals; these results are in good agreement with the collected dataset (Fig.
544 7). Thus, the benthic Cd_w results provide new evidence for tracking the northern flow of AAIW in the northern
545 Indian Ocean, which increased during HS1 and the YD.

546   Taken together, Cd_w, B-P age offset, benthic $\delta^{13}C$, ε_{Nd} and $\Delta^{14}C$ records reported from the northern Indian
547 Ocean all suggest strong upwelling and enhanced northern flow of AAIW from the Southern Ocean during HS1
548 and the YD. Thus, the variations in these records can provide strong evidence for the hypothesis that Southern
549 Ocean upwelling played a vital role in the increase of atmospheric CO_2 in the deglacial period (Anderson et al.,
550 2009; Skinner et al., 2010, 2014). However, Kohfeld et al. (2005) suggested that although physical processes
551 (such as ventilation) are involved in the glacial-interglacial atmospheric CO_2 change, the biological pump may
552 also contribute nearly half of the observed changes of CO_2 during the glacial-interglacial transitions. As shown
553 above, the HS1 event is characterized by reduced surface productivity, as revealed by the lower percentage
554 values of *G. bulloides* in core MD77-191 (Bassinot et al., 2011) and by several studies of cores located in the
555 eastern and western Arabian Sea within the Oxygen Minimum Zone (e.g., Schulz et al., 1998; Altabet et al.,
556 2002; Ivanochko et al., 2005; Singh et al., 2006, 2011; Naik et al., 2017). This reduced productivity at a
557 millennial timescale suggests that the entire biological factory was related to the reduced monsoon intensity
558 during the North Atlantic Heinrich events (e.g., Singh et al., 2011; Naik et al., 2017). Thus, a weaker biological
559 production could also have contributed to the two-step increase of atmospheric CO_2 during the last deglaciation,
560 at least for the HS1 period.

561

6. Conclusions

Changes in benthic foraminiferal Cd/Ca and assemblages were reconstructed on core MD77-191 (1254 m water depth) located off the southern tip of India, as well as on core MD77-176 (1375 m water depth) from the northern BoB, in order to reveal the evolution of intermediate water circulation and paleo-nutrient changes in the northern Indian Ocean since the last deglaciation. We reconstructed seawater Cd_w concentration by converting *H. elegans* Cd/Ca. Benthic Cd/Ca ratios are mainly influenced by changes in surface productivity and intermediate-bottom water ventilation.

Results indicate that assemblages 2 and 3, reflecting high bottom water oxygen conditions and a low flux of organic matter, dominated between 17 and 6 cal kyr BP, corresponding to a poor productivity time-period. The typical late Holocene assemblage indicates a relatively low-oxygen level and meso- to eutrophic deep-water conditions, associated with high surface productivity. The early Holocene (10-6 cal ka BP) corresponds to a low in productivity associated with depleted Cd_w in intermediate water. These observations seem to result from enhanced monsoon precipitation and increased river inputs from the Himalayan Rivers, which led to more marked stratification in the BoB and a reduction in primary and export productivity. At the southern tip of India, the decrease in vertical mixing is also associated with a reduction in summer wind forcing resulting from the northward displacement of ITCZ during summer (Bassinot et al., 2011). During the late Holocene (5.2-2.4 cal kyr BP), the increased intermediate Cd_w concentrations of cores MD77-191 and MD77-176 indicate enhanced surface productivity in the southeastern Arabian Sea and in the northeastern BoB, corresponding to weakened monsoon intensity and rainfall, in agreement with other local records and reconstructions of the paleo-monsoon strength. Thus, our results clearly show the strong control of intermediate water Cd_w during the Holocene by orbitally-driven changes in summer monsoon productivity.

As far as millennial-scale variability is concerned, during the last deglaciation, decreased intermediate Cd_w concentrations during HS1 and the YD are coeval with increased benthic $\delta^{13}C$, depletion in $[CO_3^{2-}]$ and decreased B-P age offsets. These observations indicate that the low Cd_w values in intermediate water mainly resulted from the increased northward flow of AAIW during HS1 and YD intervals. These signals also provide strong evidence for the important role of enhanced Southern Ocean ventilation in the CO_2 increase during the last deglaciation. The declined intermediate Cd_w obtained from southeastern Arabian Sea (Core MD77-191), combined with the published eastern and western Arabian Sea paleo-productivity results, together provide evidence for the important influence of decreased monsoon intensity at a millennial time scale during cold events in the North Atlantic region, associated with the increase in atmospheric CO_2 during the last deglaciation.

Data availability

All data are given in Table 1 and supplementary materials Tables S1-S2.

Supplement

The supplement related to this paper is available online.

Author contribution

RM, SS, FB and CC developed the idea and interpreted the results. CC and FB supplied foraminifera samples. RM did benthic foraminifera assemblage and geochemical analyses with the aide of FH and LL. ZY and LL

603   joined the discussion. All co-authors helped to improve the article.
604
605   **Competing interests**
606   The authors declare that they have no conflict of interest.
607
608   **Acknowledgements**

609   R. Ma gratefully acknowledges the China Scholarship Council for providing funding for her study in France.
610   The authors wish to thank one anonymous reviewer as well as André Bahr for useful suggestions and discussions
611   during the revision process. The research leading to this paper was funded by the French National Research
612   Agency under the "*Investissements d'avenir*" programme (Grant ANR-11-IDEX-0004-17-EURE-0006), and the
613   INSU-LEFE-IMAGO-CITRON GLACE project.

614
615   **References**
616

617   Almogi-Labin, A., Schmiedl, G., Hemleben, C., Siman-Tov, R., Segl, M., and Meischner, D.: The influence of
618   the NE winter monsoon on productivity changes in the Gulf of Aden, NW Arabian Sea, during the last 530ka
619   as recorded by foraminifera, Marine Micropaleontology, 40 (3), 295–319, 2000.

620   Altabet, M. A., Higginson, M. J., and Murray, R. W.: The effect of millennial-scale changes in theArabian Sea
621   denitrification on atmospheric CO_2, Nature, 415, 159–162, 2002.

622   Altenbach, A. V., Pflaumann, U., Schiebel, R., Thies, A., Timm, S., and Trauth, M.: Scaling percentages and
623   distributional patterns of benthic foraminifera with flux rates of organic carbon, Journal of Foraminiferal
624   Research, 29 (3), 173–185, 1999.

625   Anderson, R. F., Ali, S., Bradtmiller, L. I., Nielsen, S. H. H., Fleisher, M. Q., Anderson, B. E., and Burckle, L.
626   H.: Wind-driven upwelling in the Southern Ocean and the deglacial rise in atmospheric CO_2, Science, 323
627   (5920), 1443–1448, 2009.

628   Banse, K.: Seasonality of phytoplankton chlorophyll in the central and northern Arabian Sea, Deep Sea Research
629   Part A Oceanographic Research Papers, 34 (5), 713–723, 1987.

630   Barker, S., Greaves, M., and Elderfield, H.: A study of cleaning procedures used for foraminiferal Mg/Ca
631   paleothermometry, Geochemistry Geophysics Geosystems, 4 (9), 1–20, 2003.

632   Bassinot, F. C., Marzin, C., Braconnot, P., Marti, O., Mathienblard, E., Lombard, F., and Bopp, L.: Holocene
633   evolution of summer winds and marine productivity in the tropical Indian Ocean in response to insolation
634   forcing: Data-model comparison, Climate of the Past, 7 (3), 815–829, 2011.

635   Bauska, T. K., Baggenstos, D., Brook, E. J., Mix, A. C., Marcott, S. A., Petrenko, V. V., Schaefer, H.,
636   Severinghaus, J. P., and Lee, J. E.: Carbon isotopes characterize rapid changes in atmospheric carbon dioxide
637   during the last deglaciation, Proceedings of the National Academy of Sciences, 113(13), 3465–3470, 2016.

638   Beal, L. M., Ffield, A., and Gordon, A. L.: Spreading of Red Sea overflow waters in the Indian Ocean, Journal of
639   Geophysical Research: Oceans, 105 (C4), 8549–8564, 2000.

640   Bostock, H. C., Opdyke, B. N., and Williams, M. J. M.: Characterising the intermediate depth waters of the
641   Pacific Ocean using $\delta^{13}C$ and other geochemical tracers, Deep-Sea Research I, 57 (7), 847–859, 2010.

642   Boyle, E. A.: Manganese carbonate overgrowths on foraminifera tests, Geochim. Cosmochim. Acta, 63 (18),
643   353–353, 1983.

644   Boyle, E. A.: Cadmium: Chemical tracer of deepwater paleoceanography, Paleoceanography, 3 (4), 471–489,
645   1988.

646   Boyle, E. A.: Cadmium and $\delta^{13}C$ paleochemical ocean distributions during the stage 2 Glacial Maximum,
647   Annual Review of Earth and Planetary Sciences, 20 (1), 245–287, 1992.

648   Boyle, E. A. and Keigwin, L. D.: Deep circulation of the north Atlantic over the last 200,000 years: Geochemical
649   evidence, Science, 218 (4574), 784–787, 1982.

650   Boyle, E. A., Labeyrie, L., and Duplessly, J. C.: Calcitic foraminiferal data confirmed by cadmium in aragonitic
651   Hoeglundina: Application to the Last Glacial Maximum in the northern Indian Ocean, Paleoceanography, 10
652   (5), 881–900, 1995.

653   Boyle, E. A., Sclater, F., and Edmond, J. M.: On the marine geochemistry of Cadmium, Nature, 263 (5572), 42–
654   44, 1976.

655   Bryan, S. P. and Marchitto, T. M.: Testing the utility of paleonutrient proxies Cd/Ca and Zn/Ca in benthic
656   foraminifera from thermocline waters, Geochemistry, Geophysics, Geosystems, 11 (1), 2010.

657   Bryan, S. P., Marchitto, T. M., and Lehman, S. J.: The release of ^{14}C-depleted carbon from the deep ocean during
658   the last deglaciation: Evidence from the Arabian Sea, Earth and Planetary Science Letters, 298 (1), 244−254,
659   2010.

660   Burmistrova, I. I. and Belyaeva, N. V.: Bottom foraminiferal assemblages in the Deryugin Basin (Sea of
661   Okhotsk) during the past 26000 years, Oceanology, 46 (6), 834−840, 2006.

662   Came, R. E., Oppo, D. W., Curry, W. B., and Lynch-Stieglitz, J.: Deglacial variability in the surface return flow
663   of the Atlantic meridional overturning circulation, Paleoceanography, 23, PA1217, 2008.

664   Canfield, D. E.: Factors influencing organic carbon preservation inmarine sediments, Chem. Geol., 114, 315−329,
665   1994.

666   Calvert, S. E., Pedersen, T. F., Naidu, P. D., and von Stackelberg, U.: On the organic carbon maximum on the
667   continental slope of the eastern Arabian Sea, J. Mar. Res., 53, 269−296, 1995.

668   Cao, L., Fairbanks, R. G., Mortlock, R. A., and Risk, M. J.: Radiocarbon reservoir age of high latitude north
669   Atlantic surface water during the last deglacial, Quaternary Science Reviews, 26 (5), 732−742, 2007.

670   Caulle, C., Mojtahid, M., Gooday, A. J., Jorissen, F. J., and Kitazato, H.: Living (rose-bengal-stained) benthic
671   foraminiferal faunas along a strong bottom-water oxygen gradient on the Indian margin (Arabian Sea),
672   Biogeosciences, 12 (16), 5005−5019, 2015.

673   Contreras-Rosales, L. A., Jennerjahn, T., Tharammal, T., Meyer, V., Lückge, A., Paul, A., and Schefuß, E.:
674   Evolution of the Indian Summer Monsoon and terrestrial vegetation in the Bengal region during the past 18
675   ka, Quaternary Science Reviews, 102, 133−148, 2014.

676   Corliss, B. H.: Recent deep-sea benthonic foraminiferal distributions in the southeast Indian Ocean: Inferred
677   bottom-water routes and ecological implications, Marine Geology, 31 (1-2), 115−138, 1979.

678   Corliss, B. H., Martinson, D. G., and Keffer, T.: Late Quaternary deep-ocean circulation, Geological Society of
679   America Bulletin, 97 (9), 1106, 1986.

680   Curry, W. B., Duplessy, J. C., Labeyrie, L. D., and Shackleton, N. J.: Changes in the distribution of $\delta^{13}C$ of deep
681   water σCO_2 between the last glaciation and the Holocene, Paleoceanography, 3 (3), 317−341, 1988.

682   Curry, W. B., Ostermann, D. R., Guptha, M. V. S., and Ittekkot, V.: Foraminiferal production and monsoonal
683   upwelling in the Arabian Sea: evidence from sediment traps, Geological Society, London, Special
684   Publications, 64, 93−106, 1992.

685   De, S. and Gupta, A. K.: Deep-sea faunal provinces and their inferred environments in the Indian Ocean based
686   on distribution of recent benthic foraminifera, Palaeogeography, Palaeoclimatology, Palaeoecology, 291 (3),
687   429−442, 2010.

688   De Rijk, S., Jorissen, F. J., Rohling, E. J., and Troelstra, S. R.: Organic flux control on bathymetric zonation of
689   Mediterranean benthic foraminifera, Marine Micropaleontology, 40, 151−166, 2000.

690   Den Dulk, M., Reichart, G. J., Memon, G. M., Roelofs, E. M. P., Zachariasse, W. J., and Zwaan, G. J. V. D.:
691   Benthic foraminiferal response to variations in surface water productivity and oxygenation in the northern
692   Arabian Sea, Marine Micropaleontology, 35 (1–2), 43−66, 1998.

693   Duplessy, J. C., Shackleton, N. J., Matthews, R. K., Prell, W., Ruddiman, W. F., Caralp, M., and Hendy, C. H.:
694   ^{13}C record of benthic foraminifera in the last interglacial ocean: Implications for the carbon cycle and the
695   global deep water circulation, Quaternary Research, 21 (2), 225−243, 1984.

696   Eberwein, A. and Mackensen, A.: Live and dead benthic foraminifera and test $\delta^{13}C$ record primary productivity
697   off Morocco (NW-Africa), Deep-Sea Research. Part I, 53 (8), 1379−1405, 2006.

698   Eberwein, A. and Mackensen, A.: Last Glacial Maximum paleoproductivity and water masses off NW-Africa:
699   Evidence from benthic foraminifera and stable isotopes, Marine Micropaleontology, 67, 87−103, 2008.

700   Elderfield, H. and Rickaby, R. E. M.: Oceanic Cd/P ratio and nutrient utilization in the glacial Southern Ocean,
701   Nature, 405 (6784), 305−310, 2000.

702   Fontanier, C., Jorissen, F. J., Licari, L., Alexandre, A., Anschutz, P., and Carbonel, P.: Live benthic

703   foraminiferal faunas from the Bay of Biscay: Faunal density, composition, and microhabitats, Deep Sea
704   Research Part I: Oceanographic Research Papers, 49 (4), 751−785, 2002.

705   Gauns, M., Madhupratap, M., Ramaiah, N., Jyothibabu, R., Fernandes, V., Paul, J. T., and Prasanna Kumar, S.:
706   Comparative accounts of biological productivity characteristics and estimates of carbon fluxes in the Arabian
707   Sea and the Bay of Bengal, Deep-Sea Research II, 52, 2003−2017, 2005.

708   Gomes, H., Goes, J., and Saino, T.: Influence of physical processes and freshwater discharge on the seasonality
709   of phytoplankton regime in the Bay of Bengal, Continental Shelf Research, 20, 313−330, 2000.

710   Gupta, A. K. and Thomas, E.: Latest Miocene-Pleistocene productivity and deep-sea ventilation in the
711   Northwestern Indian Ocean (Deep Sea Drilling Project Site 219), Paleoceanography, 14(1), 62−73, 1999.

712   Gupta, A. K., Anderson, D. M., and Overpeck, J. T.: Abrupt changes in the Asian Southwest Monsoon during
713   the Holocene and their links to the North Atlantic Ocean, Nature, 421 (6921), 354−357, 2003.

714   Hammer, Ø., Harper, D. A. T., and Ryan, P. D.: Past: Paleontological statistics software package for education
715   and data analysis, 2001.

716   Hall, J. M. and Chan, L. H.: Ba/Ca in benthic foraminifera: Thermocline and middepth circulation in the north
717   Atlantic during the last glaciation, Paleoceanography, 19, PA4018, 2004.

718   Hermelin, J. O. R.: Relative abundances of benthic foraminifera in ODP hole 117-728A, PANGAEA, 1991.

719   Hermelin, J. O. R.: Variations in the benthic foraminiferal fauna of the Arabian Sea: A response to changes in
720   upwelling intensity? Geological Society, London, Special Publications, 64, 151−166, 1992.

721   Hermelin, J. O. R. and Shimmield, G. B.: Impact of productivity events on the benthic foraminiferal fauna in the
722   Arabian Sea over the last 150,000 years, Paleoceanography, 10 (1), 85−116, 1995.

723   Hertzberg, J. E., Lund, D. C., Schmittner, A., and Skrivanek, A. L.: Evidence for a biological pump driver of
724   atmospheric CO_2 rise during Heinrich Stadial 1, Geophysical Research Letters, 43(23), 12,242−12,251, 2016.

725   Hester, K. and Boyle, E.: Water chemistry control of Cadmium content in recent benthic foraminifera, Nature,
726   298, 260−262, 1982.

727   Holbourn, A., Henderson, A. S., and Macleod, N.: Front matter. In Atlas of benthic foraminifera, pp. 1−641,
728   2013.

729   Ivanochko, T. S., Ganeshram, R. S., Brummer, G. J. A., Ganssen, G., Jung, S. J. A., Moreton, S. G., and Kroon,
730   D.: Variations in tropical convection as an amplifier of global climate change at the millennial scale, Earth
731   Planet. Sci. Lett., 235, 302−314, 2005.

732   Jaccard, S. L., Galbraith, E. D., Mart ńez-Garc ń, A., and Anderson, R. F.: Covariation of deep Southern Ocean

733   oxygenation and atmospheric CO_2 through the last ice age, Nature, 530(7589), 207−210, 2016.

734 Jones, R. W.: The challenger foraminifera, Oxford University Press, 1994.

735 Jung, S. J. A., Kroon, D., Ganssen, G., Peeters, F., and Ganeshram, R.: Enhanced Arabian Sea intermediate
736   water flow during glacial North Atlantic cold phases, Earth and Planetary Science Letters, 280 (1), 220−228,
737   2009.

738 Kohfeld, K. E., Quéré, C. L., Harrison, S. P., and Anderson, R. F.: Role of marine biology in Glacial-interglacial
739   CO_2 cycles, Science, 308, 74, 2005.

740 Laskar, L., Robutel, P., Joutel, F., Gastineau, M., Correia, A. C., and Levrard, B.: A long-term numerical
741   solution for the insolation quantities of the Earth, Astronomy and Astrophysics, 428, 261-285, 2004.

742 Lévy, M., Shankar, D., André, J.-M., Shenoi, S., Durand, F., and De Boyer Montegut, C.: Basin-wide seasonal
743   evolution of the Indian Ocean's phytoplankton blooms, Journal of Geophysical Research, 112 (C12014), 1−
744   14, 2007.

745 Loeblich, A. R. and Tappan, H.: Generic taxa erroneously regarded as foraminifers. In Foraminiferal genera and
746   their classification, Loeblich, A. R., Tappan, H., Eds. Springer US: Boston, MA, pp. 726−730, 1988.

747 Lynch-Stieglitz, J., Fairbanks, R. G., and Charles, C. D.: Glacial-interglacial history of Antarctic Intermediate
748   Water: Relative strengths of Antarctic versus Indian Ocean sources, Paleoceanography, 9 (1), 7−29, 1994.

749 Ma, R., Sépulcre, S., Bassinot, F., Haurine, F., Tisnérat-Laborde, N., and Colin, C.: North Indian Ocean
750   circulation since the last deglaciation as inferred from new elemental ratio records for benthic foraminifera
751   *Hoeglundina elegans*, Paleoceanography and Paleoclimatology, 35, 2020.

752 Ma, R., Sépulcre, S., Licari, L., Bassinot, F., Liu, Z., Tisnérat-Laborde, N., Kallel, N., Yu, Z., and Colin, C.:
753   Changes in intermediate circulation in the Bay of Bengal since the Last Glacial Maximum as inferred from
754   benthic foraminifera assemblages and geochemical proxies, Geochemistry, Geophysics, Geosystems, 20,
755   1592−1608, 2019.

756 Mackensen, A., Hubberten, H. W., Bickert, T., Fischer, G., and Futterer, D. K.: $\delta^{13}C$ in benthic foraminiferal
757   tests of Fontbotia wuellerstorfi (Schwager) relative to $\delta^{13}C$ of dissolved inorganic carbon in Southern Ocean
758   deep water: implications for Glacial ocean circulation models, Paleoceanography, 6, 587−610, 1993.

759 Mackensen, A., Schmiedl, G., Harloff, J., and Giese, M.: Deep-sea foraminifera in the South Atlantic Ocean;
760   ecology and assemblage generation, Micropaleontology, 41 (4), 342−358, 1995.

761 Madhupratap, M., Gauns, M., Ramaiah, N., Prasanna Kumar, S., Muraleedharan, P. M., Sousa, S. N., and
762   Muraleedharan, U.: Biogeochemistry of the Bay of Bengal: physical, chemical and primary productivity
763   characteristics of the central and western Bay of Bengal during summer monsoon 2001, Deep-Sea Research
764   II, 50, 881−896, 2003.

765 Marchitto, T. M. and Broecker, W. S.: Deep water mass geometry in the glacial atlantic ocean: A review of
766   constraints from the paleonutrient proxy Cd/Ca, Geochemistry, Geophysics, Geosystems, 7, 2006.

767 Marchitto, T. M., Lehman, S. J., Ortiz, J. D., Flückiger, J., and Geen, A. V.: Marine radiocarbon evidence for the
768   mechanism of deglacial atmospheric CO_2 rise, Science, 316, 1456−1459, 2007.

769 Marra, J. and Barber, R. T.: Primary productivity in the Arabian Sea: A synthesis of JGOFS data, Progress in
770   Oceanography, 65 (2), 159−175, 2005.

771 Marzin, C., Kallel, N., Kageyama, M., Duplessy, J. C., and Braconnot, P.: Glacial fluctuations of the Indian
772   monsoon and their relationship with north Atlantic climate: New data and modelling experiments, Clim. Past,
773   9 (5), 2135−2151, 2013.

774 McCorkle, D. C., Martin, P. A., W. Lea, D. W., and Klinkhammer, G. P.: Evidence of a dissolution effect on
775   benthic foraminiferal shell chemistry: δ^{13}C, Cd/Ca, Ba/Ca, and Sr/Ca results from the ontong Java Plateau,
776   Paleoceanography, 10 (4), 699−714, 1995.

777 Mléneck, V. M.: Sédimentation et dissolution des carbonates biogéniques aux moyennes latitudes Nord et Sud,
778   Approche quantitative et relations avec les paléocirculations océaniques des derniers 150 000 ans. PhD thesis,
779   Université Bordeaux I, pp. 277, 1997.

780 Monnin, E., Indermühle, A., Dällenbach, A., Flückiger, J., Stauffer, B., Stocker, T. F., Raynaud, D., and Barnola,
781   J. M.: Atmospheric CO_2 concentrations over the last glacial termination, Science, 291 (5501), 112−114, 2001.

782 Murgese, D. S. and De Deckker, P.: The distribution of deep-sea benthic foraminifera in core tops from the
783   eastern Indian Ocean, Marine Micropaleontology, 56 (1), 25−49, 2005.

784 Murgese, D. S. and De Deckker, P.: The late quaternary evolution of water masses in the eastern Indian Ocean
785   between Australia and Indonesia, based on benthic foraminifera faunal and carbon isotopes analyses,
786   Palaeogeography, Palaeoclimatology, Palaeoecology, 247 (3), 382−401, 2007.

787 Naqvi, W. A., Charles, C. D., and Fairbanks, R. G.: Carbon and oxygen isotopic records of benthic foraminifera
788   from the northeast indian ocean: Implications on glacial-interglacial atmospheric CO_2 changes, Earth and
789   Planetary Science Letters, 121 (1), 99−110, 1994.

790 Naidu, P. D., Prakash Babu, C., and Rao, C. M.: The upwelling record in the sediments of the western
791   continental margin of India, Deep-Sea Res., 39, 715−723, 1992.

792 Naidu, P. D. and Malmgren, B. A.: A high-resolution record of late Quaternary upwelling along the Oman
793   margin, Arabian Sea based on planktonic foraminifera, Paleoceanography, 11, 129−140, 1996.

794 Naik, D. K., Saraswat, R., Lea, D. W., Kurtarkar, S. R., and Mackensen, A.: Last glacial-interglacial productivity
795   and associated changes in the eastern Arabian Sea, Palaeogeography, Palaeoclimatology, Palaeoecology, 483,
796   147−156, 2017.

797   O'Malley, R.: Ocean productivity. http://www.science.oregonstate.edu/ocean.Productivity/ index.php. 2017.

798   Olsen, A., Key, R. M., van Heuven, S., Lauvset, S. K., Velo, A., Lin, X., and Suzuki, T.: The Global Ocean Data
799   Analysis Project version 2 (GLODAPv2) – an internally consistent data product for the world ocean, Earth
800   System Science Data, 8(2), 297−323, 2016.

801   Olson, D. B., Hitchcock, G. L., Fine, R. A., and Warren, B. A.: Maintenance of the low-oxygen layer in the
802   central Arabian Sea, Deep-Sea Research Part II: Tropical Studies In Oceanography, 40(3), 673−685. 1993.

803   Oppo, D. W. and Fairbanks, R. G.: Variability in the deep and intermediate water circulation of the Atlantic
804   Ocean during the past 25,000 years: Northern Hemisphere modulation of the Southern Ocean, Earth and
805   Planetary Science Letters, 86, 1−15, 1987.

806   Pahnke, K., Goldstein, S. L., and Hemming, S. R.: Abrupt changes in Antarctic Intermediate Water circulation
807   over the past 25,000 years, Nature Geoscience, 1, 870, 2008.

808   Pahnke, K. and Zahn, R.: Southern Hemisphere water mass conversion linked with north Atlantic climate
809   variability, Science, 307 (5716), 1741−1746, 2005.

810   Pena, L. D., Goldstein, S. L., Hemming, S. R., Jones, K. M., Calvo, E., Pelejero, C., and Cacho, I.: Rapid
811   changes in meridional advection of Southern Ocean intermediate waters to the tropical Pacific during the last
812   30kyr, Earth and Planetary Science Letters, 368, 20−32, 2013.

813   Peterson, L. C.: Recent abyssal benthic foraminiferal biofacies of the eastern Equatorial Indian Ocean, Marine
814   Micropaleontology, 8 (6), 479−519, 1984.

815   Phillips, S. C., Johnson, J. E., Giosan, L., and Rose, K.: Monsoon-influenced variation in productivity and
816   lithogenic sediment flux since 110 ka in the offshore Mahanadi Basin, northern Bay of Bengal, Marine and
817   Petroleum Geology, 58, 502−525, 2014.

818   Pichevin, L. E., Reynolds, B. C., Ganeshram, R. S., Cacho, I., Pena, L., Keefe, K., and Ellam, R. M.: Enhanced
819   carbon pump inferred from relaxation of nutrient limitation in the glacial ocean, Nature, 459(7250), 1114−
820   1117, 2009.

821   Poggemann, D. W., Hathorne, E., Nuernberg, D., Frank, M., Bruhn, I., Reißig, S., and Bahr, A.: Rapid deglacial
822   injection of nutrients into the tropical Atlantic via Antarctic Intermediate Water, Earth and Planetary Science
823   Letters, 463, 118−126, 2017.

824   Prasanna Kumar, S., Madhupratap, M., Dileep Kumar, M., Muraleedharan, P. M., de Souza, S. N., Gauns, M.,
825   and Sarma, V. V. S. S.: High biological productivity in the central Arabian Sea during the summer monsoon
826   driven by Ekman pumping and lateral advection, Current Science, 81, 1633−1638, 2001.

827   Prell, W. L. and Kutzbach, J. L.: Monsoon variability over the past 150,000 years, Journal of Geophysical

828   Research Atmospheres, 92 (D7), 8411−8425, 1987.

829   Reid, J. L.: On the total geostrophic circulation of the south Pacific Ocean: Flow patterns, tracers and transports,
830   Progress in Oceanography, 16 (1), 1−61, 2003.

831   Rostek, F., Bard, E., Beaufort, L., Sonzogni, C., and Ganssen, G. M.: Sea surface temperature and productivity
832   records for the past 240 kyr in the Arabian Sea, Deep Sea Research Part II: Topical Studies in Oceanography,
833   44(6-7), 1461−1480, 1997.

834   Saraswat, R., Nigam, R., and Correge, T.: A glimpse of the Quaternary monsoon history from India and
835   adjoining seas, Palaeogeography, Palaeoclimatology, Palaeoecology, 397, 1−6, 2014.

836   Sarkar, S., Prasad, S., Wilkes, H., Riedel, N., Stebich, M., Basavaiah, N., and Sachse, D.: Monsoon source shifts
837   during the drying mid-Holocene: Biomarker isotope based evidence from the core 'monsoon zone' (CMZ) of
838   India, Quaternary Science Reviews, 123, 144−157, 2015.

839   Schlitzer, R.: Ocean data view. http://odv.awi.de, 2015.

840   Schmiedl, G., De Bovee, F., Buscail, R., Charriere, B., Hemleben, C., Medernach, L., and Picon, P.: Trophic
841   control of benthic foraminiferal abundance and microhabitat in the bathyal Gulf of Lions, western
842   Mediterranean Sea, Marine Micropaleontology, 40, 167−188, 2000.

843   Schmiedl, G., Hemleben, C., Keller, J., and Segl, M.: Impact of climatic changes on the benthic foraminiferal
844   fauna in the Ionian Sea during the last 330,000 years, Paleoceanography, 13 (5), 447−458, 1998.

845   Schnitker, D.: Deep-sea benthic foraminifers: Food and bottom water masses. In: Zahn, R., Pedersent, T. F.,
846   Kaminski, M. A., Labeyrie, L. (eds), Carbon cycling in the glacial ocean: Constraints on the ocean's role in
847   global change. NATO ASI Series (Series I: Global Environmental Change), vol 17, Springer, Berlin,
848   Heidelberg, 1994.

849   Schott, F. A. and McCreary, J. P.: The monsoon circulation of the Indian Ocean, Progress in Oceanography, 51,
850   1−123, 2001.

851   Schulz, H., von Rad, U., and Erlenkeuser, H.: Correlation between Arabian Sea and Greenland climate
852   oscillation of the past 110,000 years, Nature, 393, 54−57, 1998.

853   Shankar, D., Vinayachandran, P. N., and Unnikrishnan, A. S.: The monsoon currents in the north Indian Ocean,
854   Progress in Oceanography, 52(1):63−120, 2002.

855   Singh, A. D., Jung, S. J. A., Darling, K., Ganeshram, R., Ivanochko, T., and Kroon, D.: Productivity collapses in
856   the Arabian Sea during glacial cold phases, Paleoceanography, 26, PA3210, 2011.

857   Singh, A. D., Kroon, D., and Ganeshram, R.: Millennial scale variations in productivity and OMZ intensity in

858   the eastern Arabian Sea, Journal of the Geological Society of India, 68 (3), 369−377, 2006.

859   Skinner, L. C., Claire, W., Scrivner, A. E., and Fallon, S. J.: Radiocarbon evidence for alternating northern and

860   southern sources of ventilation of the deep Atlantic carbon pool during the last deglaciation, PNAS, 111 (15),

861   5480−5484, 2014.

862   Skinner, L. C., Fallon, S., Waelbroeck, C., Michel, E., and Barker, S.: Ventilation of the deep Southern Ocean

863   and deglacial CO_2 rise, Science, 328 (5982), 1147−1151, 2010.

864   Stuiver, M. and Grootes, P. M.: GISP2 oxygen isotope ratios, Quaternary Research, 53, 277−284, 2000.

865   Tachikawa, K. and Elderfield, H.: Microhabitat effects on Cd/Ca and $\delta^{13}C$ of benthic foramnifera, Earth and

866   Planetary Science Letters, 202, 607−624, 2002.

867   Talley, L. D., Pickard, G. L., Emery, W. J., and Swift, J. H.: Preface. In Descriptive physical oceanography

868   (sixth edition), Academic Press: Boston, pp. 1−383, 2011.

869   Thushara, V. and Vinayachandran, P. N.: Formation of summer phytoplankton bloom in the northwestern Bay of

870   Bengal in a coupled physical-ecosystem model, Journal of Geophysical Research: Oceans, 121 (12), 8535−

871   8550, 2016.

872   Toggweiler, J. R.: Variation of atmospheric CO_2 by ventilation of the ocean's deepest water, Paleoceanography,

873   14, 571−588, 1999.

874   Umling, N. E., Thunell, R. C., and Bizimis, M.: Deepwater expansion and enhanced remineralization in the

875   eastern equatorial Pacific during the Last Glacial Maximum, Paleoceanography and Paleoclimatology, 33,

876   563−578, 2018.

877   Valley, S., Lynch-Stieglitz, J., and Marchitto, T. M.: Timing of deglacial AMOC variability from a high-

878   resolution seawater Cadmium reconstruction: Timing deglacial upper amoc variability, Paleoceanography, 32,

879   1195−1203, 2017.

880   Vinayachandran, P. N., Murty, V. S. N., and Ramesh Bahu, V.: Observations of barrier layer formation in the

881   Bay of Bengal during summer monsoon, Journal of Geophysical Research, 107, 8018, 2002.

882   Van der Zwaan, G. J., Duijnstee, I. A. P., Den Dulk, M., Ernst, S. R., Jannink, N. T., and Kouwenhoven, T. J.:

883   Benthic foraminifers: Proxies or problems? A review of paleocological concepts, Earth-Science Reviews, 46

884   (1), 213−236, 1999.

885   Xie, R. C., Marcantonio, F., and Schmidt, M. W.: Deglacial variability of Antarctic Intermediate Water

886   penetration into the north Atlantic from authigenic Neodymium isotope ratios, Paleoceanography, 27,

887   PA3221, 2012.

888   Yu, Z., Colin, C., Ma, R., Meynadier, L., Wan, S., Wu, Q., Kallel, N., Sepulcre, S., Dapoigny, A., and Bassinot,
889   F.: Antarctic Intermediate Water penetration into the northern Indian Ocean during the last deglaciation,
890   Earth and Planetary Science Letters, 500, 67−75, 2018.

891   Yu, J., Menviel, L., Jin, Z. D., Thornalley, D. J. R., Foster, G. L., Rohling, E. J., McCave, I. N., McManus, J. F.,
892   Dai, Y., Ren, H., He, F., Zhang, F., Chen, P. J., and Roberts, A. P.: More efficient North Atlantic carbon
893   pimp during the Last Glacial Maximum, Nat. Commun., 10, 2019.

894   Zhou, X., Duchamp-Alphonse, S., Kageyama, M., Bassinot, F., Beaufort, L., and Colin, C.: Dynamics of
895   primary productivity in the northeastern Bay of Bengal over the last 26 000 years, Clim. Past Discuss., in
896   review, 16, 1969-1986, 2020.

897   Ziegler, M., Diz, P., Hall, I. R., and Zahn, R.: Millennial-scale changes in atmospheric CO_2 levels linked to the
898   Southern Ocean carbon isotope gradient and dust flux, Nature Geoscience, 6, 457−461, 2013.

899
900
901
902
903
904
905
906
907
908
909
910
911
912
913
914
915
916
917
918
919
920
921
922
923
924
925

926   **Table 1.** Species composition of benthic foraminiferal assemblages from core MD77-191.

	Dominant species		Important associated species		Variance (%)
PC1					42
Positive loadings	*Bulimina aculeata*	0.84	*Pullenia bulloides*	0.18	
	Cibicidoides pachyderma	0.19	*Ehrenbergina trigona*	0.13	
Negative loadings	*Hoeglundina elegans*	-0.14	*Cibicidoides wuellerstorfi*	-0.04	
	Bulimina manginata	-0.07	*Globocassidulina subglobosa*	-0.06	
PC2					19
Positive loadings	*Sphaeroidina bulloides*	0.42	*Gyroidinoides orbicularis*	0.17	
	Bulimina mexicana	0.11	*Gyroidinoides soldanii*	0.07	
Negative loadings	*Bulimina aculeata*	-0.14	*Hoeglundina elegans*	-0.62	
	Cibicidoides pachyderma	-0.07			

927
928

929

930

931
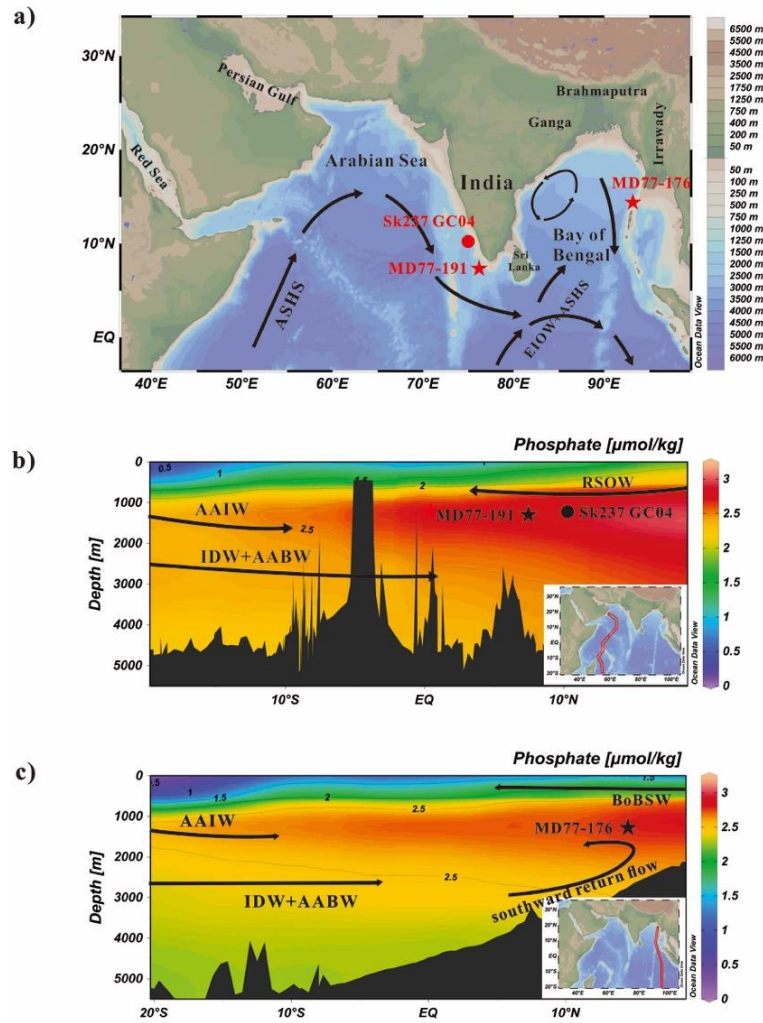
Fig. 1. (a) Oceanographic setting and locations of core MD77-191 in the Arabian Sea (red star), core MD77-176 in the Bay of Bengal (red star) and reference site SK237 GC04 (red circle, Naik et al., 2017). The black arrows represent the general surface circulation direction in the Northern Indian Ocean during the summer, Southwest Monsoon (Schott and McCreary, 2001). (b) and (c) Phosphate distribution along depth-latitude sections during the Southwest Monsoon and Northeast Monsoon periods, for the Arabian Sea and the Bay of Bengal, respectively. Data (in µmol/kg, colored scale) were contoured and plotted using the Ocean Data View (ODV) software (Schlitzer, 2015). On these two figures are shown the distribution and circulation of water masses in the Arabian Sea and Bay of Bengal (black arrows). ASHS: Arabian Sea High Salinity Water, EIOW: Eastern Indian Ocean Water, BoBSW: Bay of Bengal surface waters, AAIW: Antarctic Intermediate Water, RSOW: Red Sea Overflow Water, AABW: Antarctic Bottom Water, IDW: Indian Deep Water.
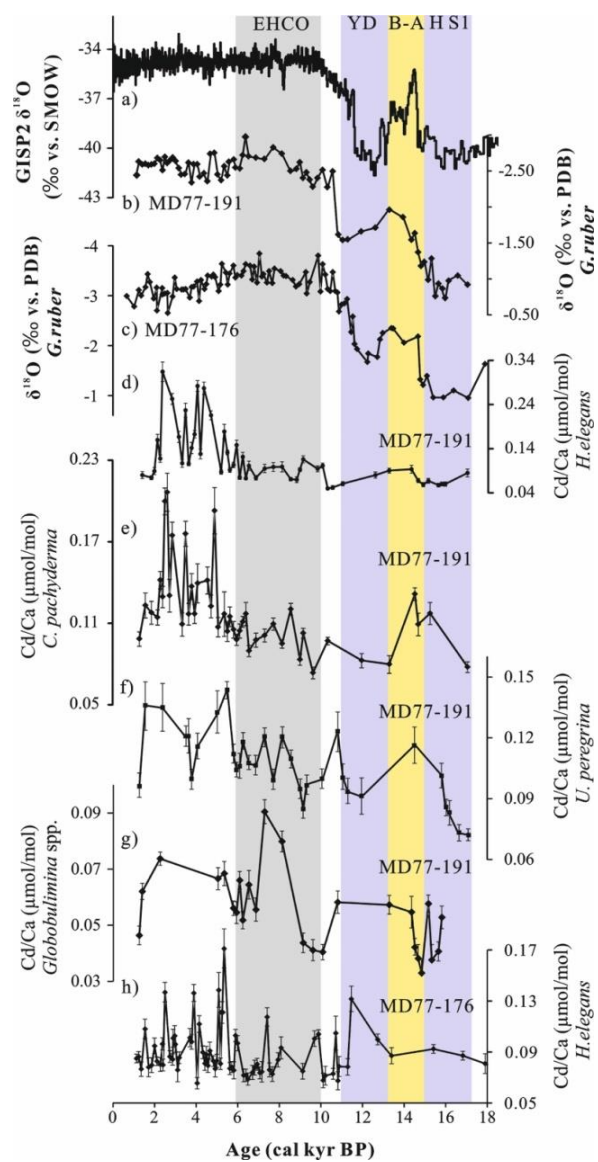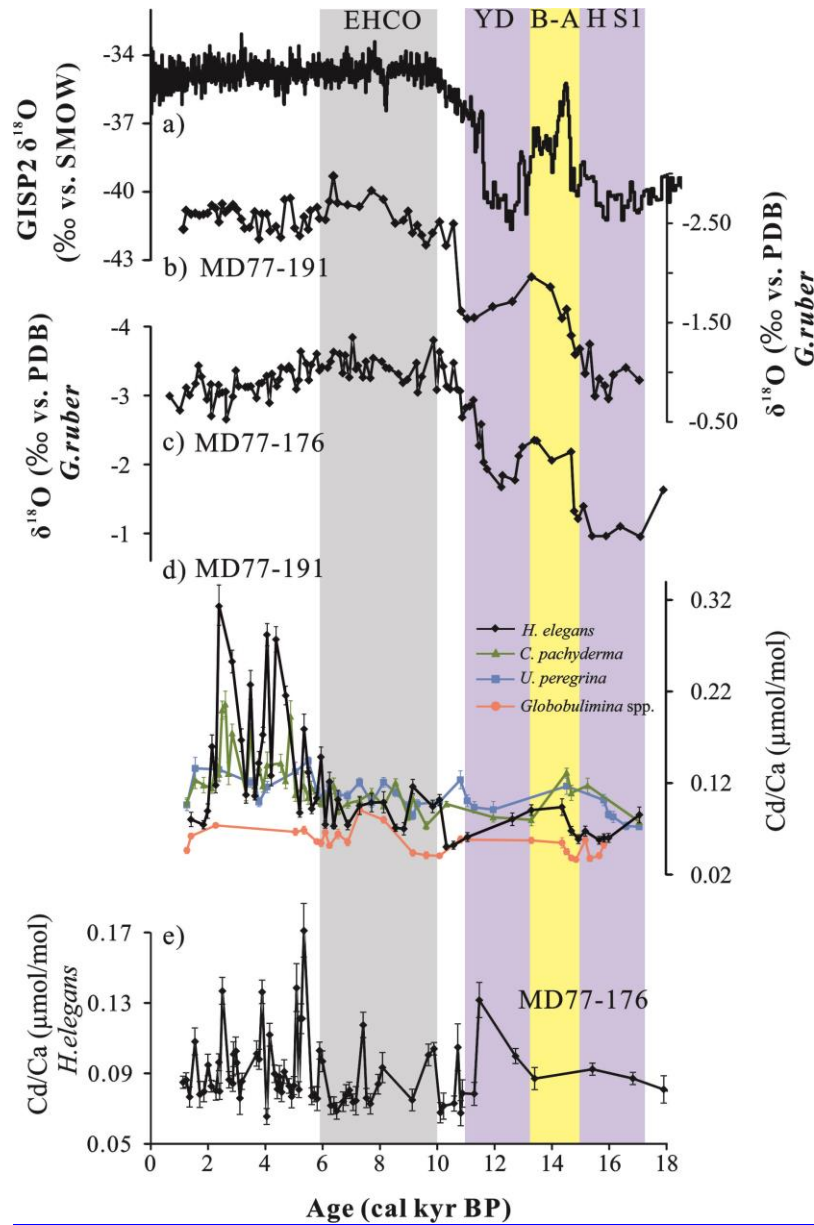
Fig. 2. (a) GISP2 Greenland ice core $\delta^{18}O$ signal (Stuiver and Grootes, 2000). (b)-(c) *Globigerinoides ruber* $\delta^{18}O$ records of cores MD77-191and MD77-176, respectively (Marzin et al., 2013; Ma et al., 2020). (d) ~~(g)~~ Cd/Ca records of the benthic foraminifera *Hoeglundina elegans* (black), *Cibicidoides pachyderma* (green), *Uvigerina peregrina* (blue), and *Globobulimina* spp. (orange) obtained from core MD77-191; (~~h~~e) Cd/Ca records of the benthic foraminifera *H. elegans* from core MD77-176. EHCO for Early Holocene Climate Optimum, YD for Younger Dryas, B-A for B∅lling-Aller∅d and HS1 for Heinrich stadial 1.

- 29 -

951

952
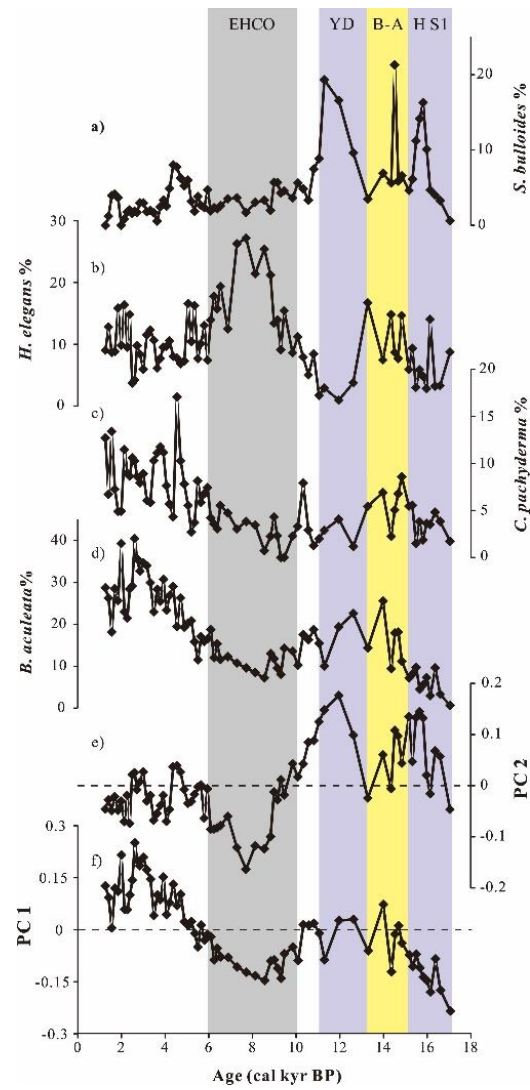
953 **Fig. 3.** Down core variations of PC scores and the percentages of major species. The color shaded intervals and

954 abbreviations are the same as in Figure 2.

955

956

957
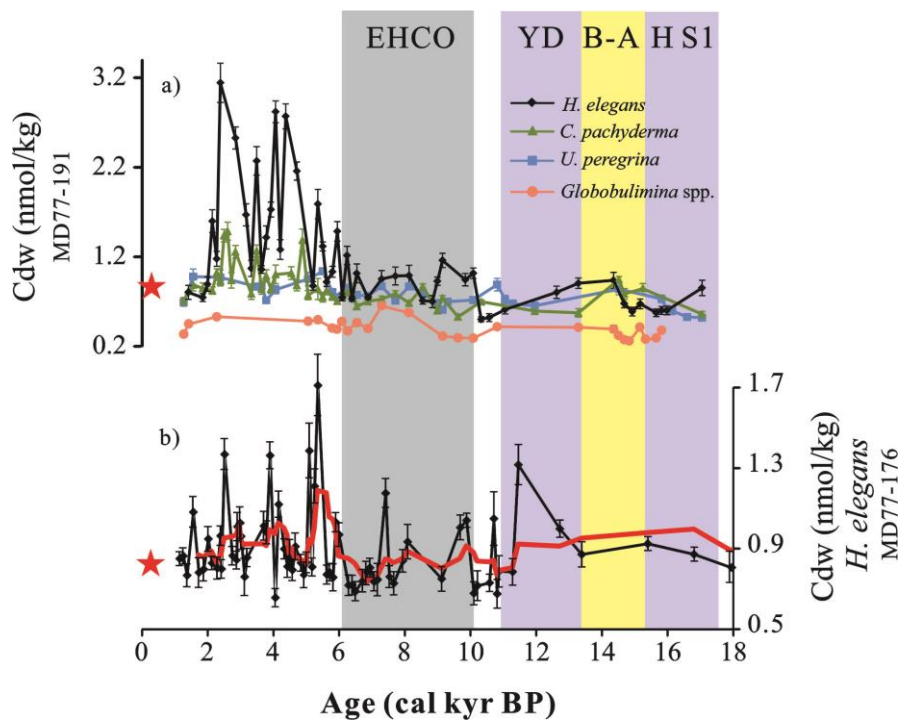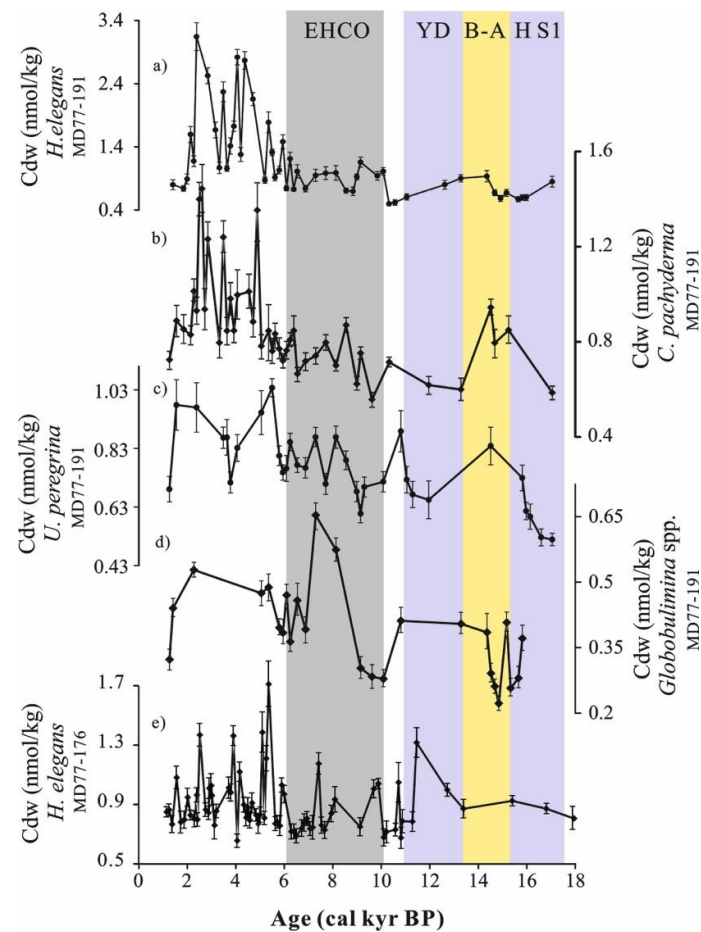
Fig. 4. (a) (d) Cd_w records calculated based on the Cd/Ca of benthic foraminifera *Hoeglundina elegans* (black), *Cibicidoides pachyderma* (green), *Uvigerina peregrina* (blue), and *Globobulimina* spp. (orange) obtained from core MD77-191, (e b) Cd_w record from core MD77-176 reconstructed using *H. elegans* Cd/Ca, the red line is the

smoothed curves using a five-point average. The red stars represent the modern Cd_w (~0.83 nmol/kg) in the northern Indian Ocean (Boyle et al., 1995). The color shaded intervals and abbreviations are the same as in Figure 2.

989

990
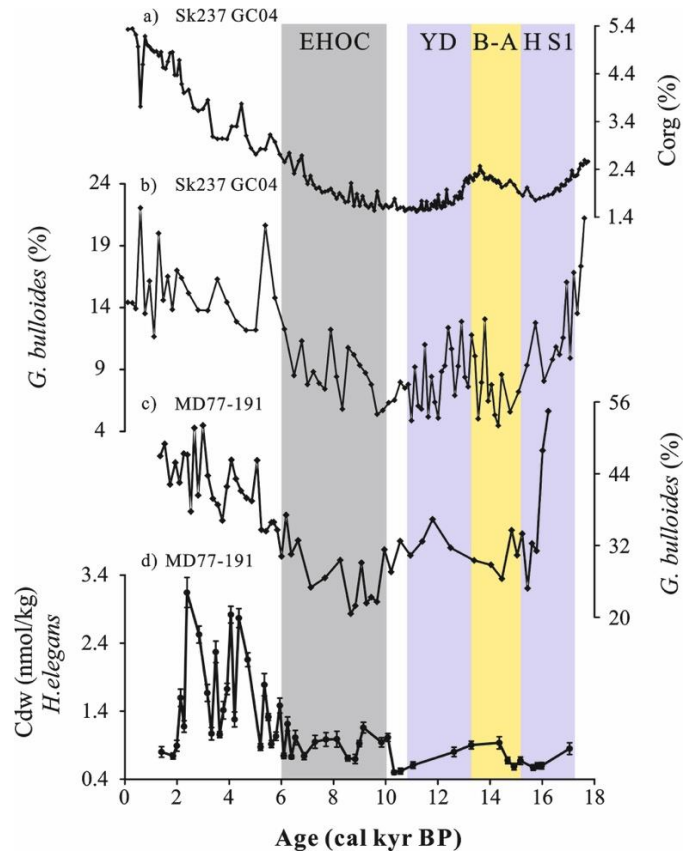
991 **Fig. 5.** (a) Organic carbon weight percentage (%C_{org}) and (b) *G. bulloides* percentage from core SK237 GC04

992 (1245m, Arabian Sea, Naik et al., 2017). (c) Relative abundance of *G. bulloides* (Mléneck, 1997; Bassinot et al.,

993 2011) and (d) Cd_w records from core MD77-191 (Arabian Sea). The color shaded intervals and abbreviations are

994 the same as in Figure 2.

995
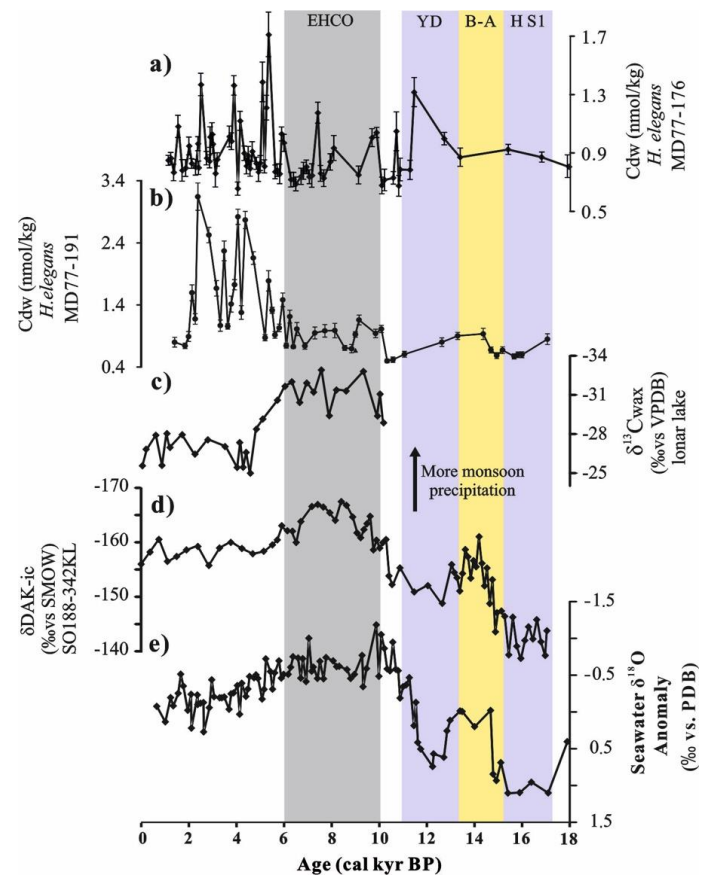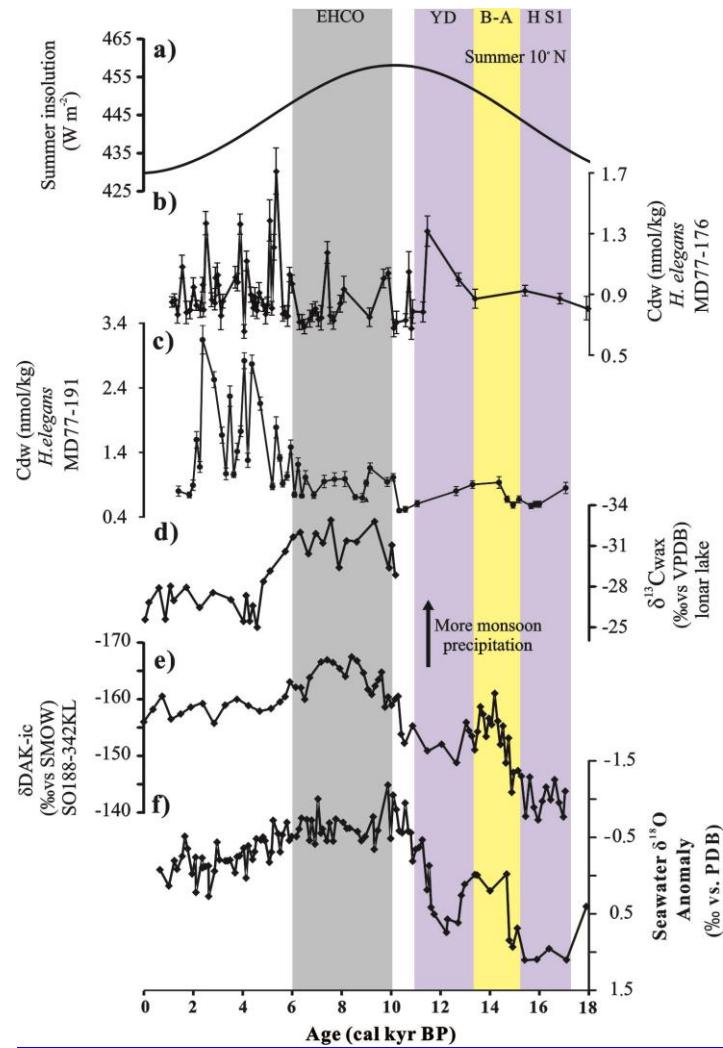
Fig. 6. (a) The solar insolation at 10°N in summer (Laskar et al., 2004). (b) and (c) intermediate Cd_w calculated from *H. elegans* obtained from MD77-176 and MD77-191, respectively. (d) Lonar Lake $\delta^{13}C_{wax}$ record (Sarkar et al., 2015). (e) δD_{Alk-ic} record from core SO188-342KL (Contreras-Rosales et al., 2014). (f) Seawater $\delta^{18}O$ anomaly obtained from MD77-176 (Marzin et al., 2013). The color shaded intervals and abbreviations are the same as in Figure 2.

1007

1008
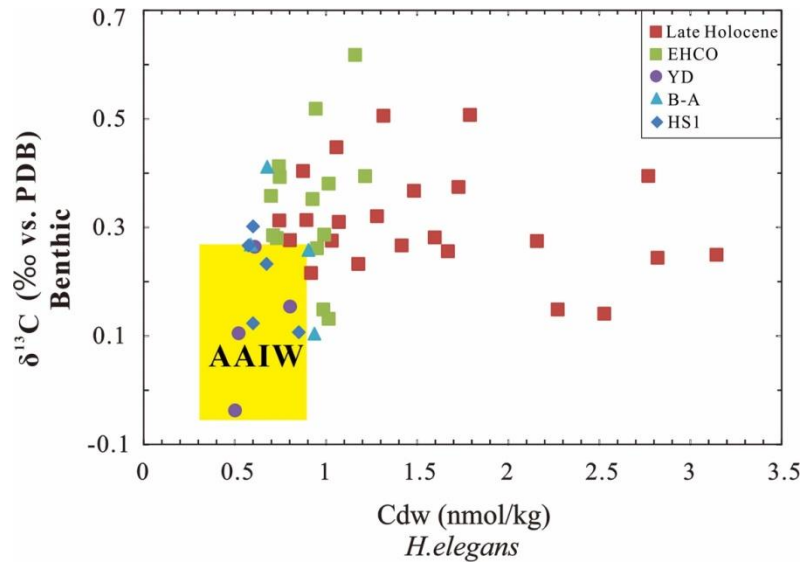
1009 **Fig. 7.** Intermediate Cd_w versus benthic $\delta^{13}C$ obtained from core MD77-191 located off the southern tip of India.

1010 The yellow shaded area represents the ranges of Cdw-$\delta^{13}C$ values of AAIW during the HS1 and YD, which were

1011 reconstructed in the Indian Ocean (benthic $\delta^{13}C$, Naqvi et al., 1994; Jung et al., 2009; Ma et al, 2019; 2020),

1012 Pacific and Atlantic Oceans (benthic Cd_w, Valley et al., 2017; Umling et al., 2018) at intermediate water depths.

1013 The abbreviations are the same as in Figure 2.